Suspended Sediment Sampling and Annual Sediment Yield on the Lower Brazos River

University of Houston, Houston, Texas

PI: Kyle Strom, Assistant Professor
Civil and Environmental Engineering

Submitted To: Texas Water Development Board
Research Project: 1000011085, 1100011340
Research Report: Final Report

February, 2013

2013 APR 11 AM 8:49
CONTRACT ADMINISTRATION

Suspended Sediment Sampling and Annual Sediment Yield on the Lower Brazos River

University of Houston, Houston, Texas

PI: Kyle Strom, Assistant Professor
Civil and Environmental Engineering

Submitted To: Texas Water Development Board
Research Project: 1000011085, 1100011340
Research Report: Final Report

February, 2013

Suspended Sediment Sampling and Annual Sediment Yield on the Lower Brazos River

Kyle Strom[1] and Mohamad Rouhnia[2]

Final Report
Sponsor Research Project ID: 1000011085, 1100011340
Research Project Title:"Suspended Sediment Sampling and Annual Sediment Yield on the Lower Brazos River"
Sponsored by Texas Water Development Board

November, 2012

Department of Civil and Environmental Engineering
University of Houston
Houston, Texas 77204-4003

[1]Assistant Professor, Civil and Environmental Engineering, University of Houston, Houston, Texas 77204-4003, phone: (713) 743-2774, e-mail: kbstrom@uh.edu
[2]Graduate Research Assistant, Civil and Environmental Engineering, University of Houston.

Abstract

This report presents measured sediment transport data and an effective discharge analysis for six USGS gage stations along the Brazos River between Waco, TX and Rosharon, TX. Measurements of channel cross-sectional properties, bed sediment grain-size distribution, suspended sediment concentration, and suspended sediment grain size distribution were made between October 2011 and July 2012 over a range of low to high flow conditions. Sediment rating curves for suspended load (measured) and bed load (calculated) and SAMwin calculated total load are developed and used in combination with USGS measured flow rates and historic sediment data to facilitate the calculation of the effective discharge and the sediment half-load discharge at each station. Effective discharge is computed using two different methods for developing the pdf of the mean daily flow and using two different methods for obtaining the total bed material load; i.e., one using the rating curves for the measured suspended load and calculated bed load, and one using a simple Engelund and Hansen total load equation to calculate both bed and suspended load in the software package SAMwin. The effective discharge and half-load transport values are compared to the pure flow metrics of bankfull flow and the 1.5 year return period flow. Overall, it is found that the effective discharge can be calculated using only the measured suspended bed material load rating curve (bed load is negligible in the calculation) and that identical effective discharges can be calculated using only the Engelund and Hansen total load equation in SAMwin with the measured bed material grain size distribution and channel cross sectional properties. Progressing downstream from Waco to Rosharon, the calculated effective discharge varies less systematically than the half-load discharge. In general, the half-load discharge is found to be approximately equal to the bankfull discharge, with the exception of the Rosharon crossing. Whereas, the effective discharge is approximately equal to the bankfull discharge at the Waco, Richmond, and Rosharon crossings, and is significantly different than the bankfull discharge at Highbank, Bryan, and Hempstead. In general, the 1.5 year return period discharge is equal to or slightly greater than the bankfull discharge and half-load discharge. Yearly sediment yields of bed load, suspended bed material load, and total suspended sediment load (bed material + wash load) are reported for each station using the USGS flow data from January 1, 1990 to December 31, 2009 and the computed rating curves for each transport mode and station.

Disclaimer

The contents of this report reflect the views of the author(s), who is (are) responsible for the facts and the accuracy of the data presented herein. The contents do not necessarily reflect the official view or policies of Texas Water Development Board. This report does not constitute a standard, specification, or regulation. This report is not intended for construction, bidding, or permit purposes. Trade or manufacturers names appear herein solely because they are considered essential to the object of this report. The researcher in charge of the project was Dr. Kyle Strom at the University of Houston.

Acknowledgements

University of Houston researchers Kyle Strom and Mohamad Rouhnia would like to acknowledge and thank Nolan Raphelt and Mark Wentzel of the TWDB for their cooperation, guidance, and support of the project. Mehrdad Salehi contributed significantly to the project during is PhD studies at the University of Houston. We would also like to thank the following graduate and undergraduate students for their help with sample collection and processing: Ali Keyvani, Guillermo Machado, Miguel Albuja, Frederick Ma, Daniel Timme, and Paul Hamilton.

Contents

List of Figures

List of Tables

1 Introduction

This report covers TWDB projects 1000011085 and 1100011340.

1.1 Project goal and objectives

The goal of the project was to develop annual sediment yield and effective discharge estimates for six gaging stations along the Brazos River from Waco, TX to Rosharon, TX. The work was be performed in cooperation with the Instream Flow Team of the Texas Water Development Board (TWDB) and focused on obtaining field measurements of sediment transport at each gaging site over a range of flow conditions. The collected data was then used as to developing annual sediment yield and effective discharge estimates at each station. The specific objectives of the project were to:

1. Collect suspended sediment measurements and local river cross sectional data that can be used to develop sediment rating curves at the following USGS gage stations.

   (a) 08096500 - Brazos River at Waco, TX

   (b) 08098290 - Brazos River near Highbank, TX

   (c) 08108700 - Brazos River at SH 21 nr Bryan, TX

   (d) 08111500 - Brazos River near Hempstead, TX

   (e) 08114000 - Brazos River at Richmond, TX

   (f) 08116650- Brazos River near Rosharon, TX

2. Develop sediment rating curves based on the field measurements, and integrate these results with the flow frequency curve to produce sediment yield histograms and effective discharge estimates at each of the gaging stations along with calculations of sediment yield over the time period of analysis.

3. Present the work in a written report, scientific journal, and technical conference.

1.2 Overview of approach

Sediment rating curves are site-specific relations that give sediment daily discharge as a function of daily water discharge at a particular river location. The site-specific nature of such relations requires that field measurements of sediment discharge be made over a range of flow conditions, at the location of interest, for the development of the rating curves. Obtaining this data can be difficult and time intensive. This project focuses on collecting suspended sediment samples over a range of flow conditions at each of the six gaging sites listed under objective 1. Collecting bedload samples is out of the scope of this project; instead, bedload is estimated at each station using measured cross sectional data, sampled bed material, and bedload discharge relations. The measured suspended sediment load is used to develop the rating curves which

give suspended sediment load in tons per day as a function of mean daily flow. The rating curves are then used along with the calculated bedload and the flow frequency histograms developed from USGS data at each gage to produce sediment yield histograms from which the effective discharge for each station is determined (objective 2); the effective discharge is defined as the mean of the discharge increment that transports the largest fraction of the annual sediment load over a period of 20 years (January 1, 1990 to December 31, 2009). Sediment yield is then computed for each station by year using the historic daily mean flow data and the developed rating curves (objective 2). This report summarizes the methods, data, and results of the study (objective 3).

1.3 Study sites

The six gaging station sites along the Brazos are shown below in figures 1.1 through 1.3.

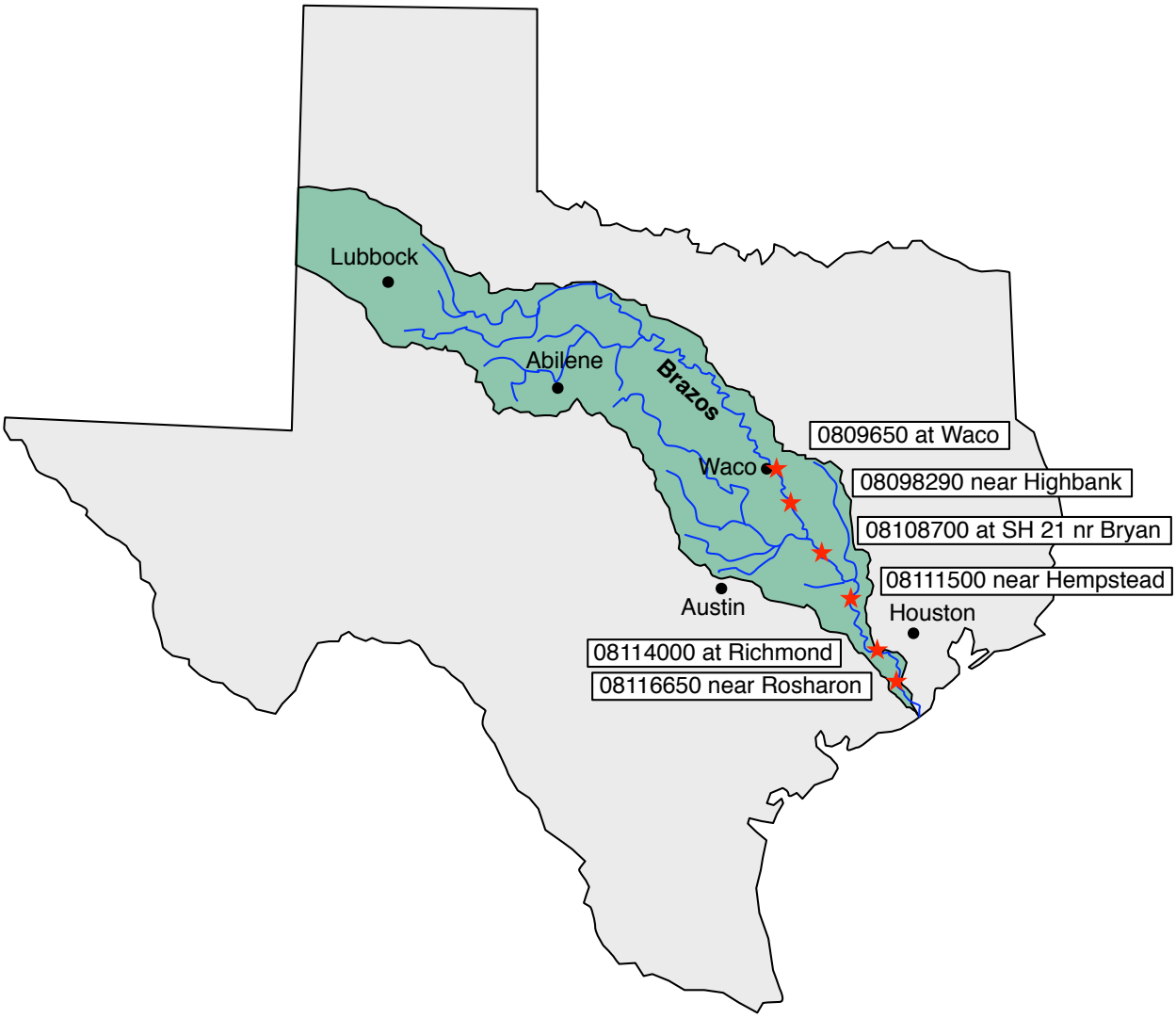

Figure 1.1: A map of Texas showing the Brazos watershed and the study gaging stations.

Figure 1.2: Pictures of the Brazos from each the study bridges near the gaging stations. (A-B) Waco 0809650 (Google Map image), (C-D) Highbank 08098290 (Google Map image), (E-F) Bryan 08108700. All photos are taken looking upstream during various low flow conditions.

Figure 1.3: Pictures of the Brazos from each of the study bridges near the gaging stations. (A-B) Hempstead 08111500, (C-D) Richmond 08114000, (E-F) Rosharon 08116650 (Google Map image). All photos are taken looking upstream during various low flow conditions.

2 Background

2.1 Effective discharge

Rivers are dynamic entities that self organize in response to imposed tectonic and climatic forces. The concept of a river at "grade" formally put forward by Mackin (1948) is useful for helping to building a framework from which to understand the trajectory of a river with time in response to the imposed boundary conditions. The grade concept simply states that a river reach will modify its slope, through vertical aggradation or degradation and/or lateral change, in such a way as to transport all of the imposed sediment at a given water discharge. This idea was built upon by Lane (1955) who parameterized the concept of a stream at grade as having,

$$QS \propto Q_S d \tag{2.1}$$

where Q is a characteristic dominant volumetric water discharge, S is the channel slope at grade, Q_S is the total bed material sediment load (bed load + suspended load), and d is the characteristic sediment grain size. Such a relationship would indicate that if, for example, slope increased due to tectonic uplift, then either or both the sediment load and size would need to increase at the given water discharge to produce a stream at an equilibrium grade. Or, if sediment load increases but discharge stays constant, the stream would respond by steepening its slope with time (Fig. 2.1). In the transition from one equilibrium state to another, a channel will adjust to the new conditions until the channel comes into a new dynamic equilibrium about the graded state where, on average, there is neither net degradation or aggradation in the channel, i.e., the same volume of sediment leaves the reach as enters it. (Fig. 2.1).

Inherent in the concept of a graded river and the Lane formulation is the notion that the river is responding to some characteristic channel-forming discharge, and that the river itself is alluvial and free to deform its boundaries through erosion of past deposits or deposition of current sediment loads. While a river can be conceptualized as morphologically responding to some characteristic constant discharge, the discharge in natural rivers continually varies over a

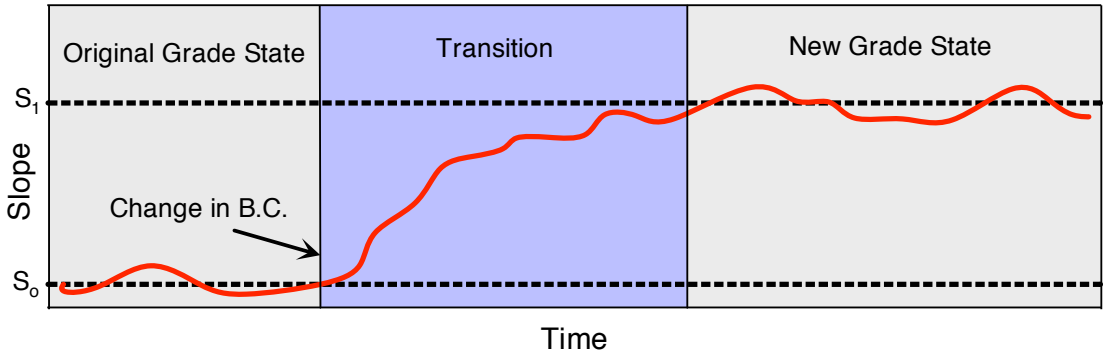

Figure 2.1: Schematic example of a channel adjusting its slope from S_o to S_1 in response to a change in bed material load, Q_b.

range of flow conditions, and one is faced with the question of, "what is the dominant channel-forming discharge that the river is morphologically responding to?" This dominant discharge is typically taken to be either the bankfull flow or the effective discharge. The bankfull flow is the discharge that just fills the channel to its banks (identified by a slope break in the stage discharge curve), and the effective discharge is defined as the discharge which moves the greatest percentage of bed material in a river over a given period of time (Wolman and Miller, 1960; Biedenharn et al., 2000). Another way to think about the effective discharge concepts is as, the discharge that does the most geomorphic work or the discharge that has the most "geomorphic effectiveness" (Wolman and Miller, 1960). Often these two characteristic discharges (bankfull and effective) are fairly close in magnitude and often have return periods on the order of 1 to 2 years (Andrews, 1980; Whiting et al., 1999; Emmett and Wolman, 2001), though they do not necessarily have to be similar (e.g., Pickup and Warner, 1976). Another measure of the dominant discharge of a river is the half-load discharge, $Q_{1/2}$, of Vogel et al. (2003), which is defined as the flow above and below which one half of the total bed material load is transported over a given time period. The half-load discharge is typically associated with a higher magnitude and longer return period flow than the effective discharge (Vogel et al., 2003; Klonsky and Vogel, 2011).

2.2 Calculating effective discharge

Various methods have been used to calculate the conceptualized effective discharge (Wolman and Miller, 1960; Sichingabula, 1999; Crowder and Knapp, 2005; Lenzi et al., 2006; Klonsky and Vogel, 2011). The most often used method is the one proposed by Wolman and Miller (1960), where the probability density function (pdf) or histogram of the daily mean flow is multiplied by the average sediment load to produce a histogram of sediment loads, $S_h = S_h(Q)$, that represents the fraction of load carried by a given discharge, Q, over the time interval of interest,

$$S_h = Q_s f_Q \tag{2.2}$$

where, $Q_s = Q_s(Q)$ is the daily sediment load (in tons per day) associated with the daily discharge value of Q, and f_Q is the pdf of the daily flow discharges (percent of time that the flow was at a rate of Q). Q_s is the total sediment bed material load and includes contributions from both bed load, Q_b, and suspended load Q_{sbm}. Sediment load histograms of the form of S_h (equation 2.2) can be developed for suspended and bed material load independently and then added together for determination of the effective discharge (Andrews, 1980; Biedenharn et al., 2000), or they can be based solely on suspended material if the transport mode is suspension dominated (Wolman and Miller, 1960; Sichingabula, 1999); often times, the analysis is done using only the suspended load because suspended load is typically the only data easily available (e.g., Klonsky and Vogel, 2011). Typically, in developing the sediment load histogram, S_L, a rating rating curve that gives the average sediment load as a function of discharge, $Q_s = Q_s(Q)$, is developed from historic or measured data using regression. The sediment load rating curve take the form of:

$$Q_s = \alpha Q^{\beta} \tag{2.3}$$

where α and β are site-specific coefficients that can be obtained through regression of the Q_s and Q paired data. Once α and β are obtained, the sediment rating equation can be used with

the pdf of the daily flow data to produce a histogram that shows the distribution of the percentage of total sediment load as a function of flow rate following equation 2.2 (fig. 2.2). The effective discharge is then selected as the flow rate, Q, associated with the peak in the S_h histogram.

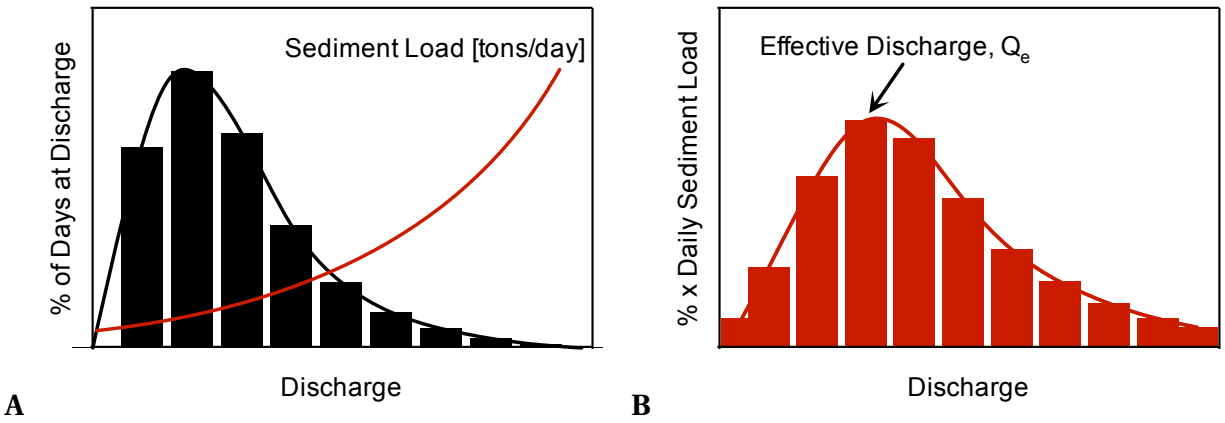

Figure 2.2: Example of a flow duration histogram (A) and a sediment load histogram (B).

Practically, f_Q is typically constructed as discrete histogram and not a continuous function. When this is the case, the discharge values used in equation 2.2 are those associated with the mid point of each discharge histogram bin (fig. 2.2A), and the effective discharge, Q_e, is the discharge of the mid point of the bin associated with the peak of the histogram.

2.3 Methods for constructing the PDF of the daily flow data

One of the biggest sources of variability in the calculation of the effective discharge comes through the way in which the pdf of the daily flow data, f_Q (also known as the flow frequency and flow duration histogram) is produced (Sichingabula, 1999; Biedenharn et al., 2000; Crowder and Knapp, 2005; Lenzi et al., 2006; Ma et al., 2010; Klonsky and Vogel, 2011). The flow frequency distribution is produced using historical measurements of the discharge over a substantial amount of time (10 or more years if possible); the discharges can be 15-minute, 1-hour, or mean daily data. The discharges are then binned and the percentage in each bin is calculated to create f_Q. Typically, the width of the bins is set manually, and some adjustment to the bin widths may be required to keep the peak in the sediment discharge histogram from occurring in the first bin (Biedenharn et al., 2000). Manual selection of the bin width is based on past experience and some general guidelines such as, starting out by sorting the flow into 25 arithmetically even-spaced bins (Hey, 1997; Biedenharn et al., 2000) and then adjusting bin number/width as needed. In the end, the exact bin number/width used is the result of trial and error, where the bin numbers are iteratively adjusted until a relatively smooth rising and falling of the sediment histogram has been developed. Developing a representative histogram or pdf of the discharge is a key since the shape of the curve, which is determined by bin number/width selection and the historical data, greatly influences the calculation of effective discharge.

Because the effective discharge calculation is dependent on the way in which the pdf of the flow data is built, methods have been sought to remove a degree of subjectiveness in cre-

ation of the flow frequency distribution. One of the more prominent methods does this through use of the kernel density function (Klonsky and Vogel, 2011). The kernel density function is non-parametric way to estimate the pdf of a random variable, in this case the mean daily discharge over a range of time. In their study, Klonsky and Vogel (2011) demonstrated that the kernel density function was a viable method for objectively evaluating both the effective and half-load discharges.

For calculating the effective discharge on the Brazos, this study uses both the traditional method of manually selecting the width of the discharge bins for the development of the flow frequency histogram and the non-parametric kernel disunity function of Klonsky and Vogel (2011).

3 Methods

3.1 Data needed

The effective discharge and annual sediment yield calculations require (1) historic discharge data for development of the daily flow pdf and (2) sediment load data for the development of sediment rating curves for each gaging station (eq. 2.3). Q_s in equation 2.3 is defined as the total bed material load, which is equal to the bed material load moving in suspension plus the bed material load moving in contact with the bed region, i.e. the bed load. Development of sediment rating curves for each station was done using physical measurements of the suspended sediment load and calculation of the bed load using bed load equations and measured cross sectional properties of the channel similar to that of Andrews (1980) and Biedenharn et al. (2000). Therefore, data needed to define Q_s at a given flow rate included: measurement of the cross-sectionally averaged suspended sediment concentration, measurement of the grain size distribution of the sediment in suspension, measurement of the channel cross-sectional geometry and cross-sectional flow area, the bed material grain size distribution, the reach slope, and the flow discharge.

3.2 Flow conditions and historic flow statistics

The data needed was collected at six different flow conditions covering a range of high, moderate, and low flow conditions at each of the six sites. The relative magnitude of high, moderate, and low flow at each site were based on exceedance values of historic, daily-mean discharge data obtained from the USGS National Water Information System (NWIS) from January 1, 1990 to December 31, 2009. For the study, high, moderate, and low flow were defined as follows: a high flow is a discharge that has historically been exceeded less than 20 percent of the time; moderate flow is a discharge that has historically been exceeded between 20 and 50 percent of the time; and low flow is a discharge that has historically been exceeded between 50 to 90 percent of the time. Of the six measurements planned per gaging site, two were made at high flow conditions, two at moderate flow conditions, and two at low flow conditions (table 3.1). The specific discharge values at the cuts of 90, 50, and 20 percent of the time exceeded for each of the six sites can be found in Table 3.2.

Sites	# of Samples	Relative Flow Magnitude	Flow Exceedance Condition
All 6 sites	2	High	Q exceeded $\leq 20\%$
All 6 sites	2	Moderate	$20\% \leq Q$ exceeded $\leq 50\%$
All 6 sites	2	Low	$50\% \leq Q$ exceeded $\leq 90\%$

Table 3.1: Sampling conditions. Six measurements per station.

	20 Years of Record						All Years of Record		
	Exceedance Values			Return Periods			Return Periods		
	$Q_{90\%}$ [cfs]	$Q_{50\%}$ [cfs]	$Q_{20\%}$ [cfs]	$Q_{1.5}$ [cfs]	Q_2 [cfs]	Q_{10} [cfs]	$Q_{1.5}$ [cfs]	Q_2 [cfs]	Q_{10} [cfs]
Waco - 0809650	90	440	1,290	16,300	20,400	40,800	24,800	33,700	104,929
Highbank - 08098290	140	710	3,000	20,000	29,824	44,300	21,200	29,500	55,491
Bryan - 08098290	195	1,080	4,340	28,800	48,600	79,411	28,800	48,600	79,411
Hempstead - 08111500	550	2,715	10,350	45,900	56,176	105,443	40,700	52,000	102,844
Richmond - 0811400	425	2,665	10,780	51,400	54,438	86,986	44,500	55,800	88,235
Rosharon - 08116650	525	3,370	12,000	46,300	55,257	81,800	44,000	51,600	78,633

Table 3.2: Discharge statistics for the percent of time exceeded ($Q_{90\%}$, $Q_{50\%}$, and $Q_{20\%}$) along with the 1.5, 2, and 10 year return period flows calculated by ranking and linear interpolation using available USGS data for the 20 year analysis time period and using all available data.

3.3 Monitoring and predicting flow conditions

Obtaining enough lead time to get out and sample the suspended sediment at the gaging stations was an important element of the project. To help with this, some simple guidelines were developed to keep track of current conditions and predict likely flow conditions at each of the stations. The simple guidelines were based on monitoring of the realtime data coming from the USGS gaging stations and monitoring of the predicted and measured rainfall over the lower watershed.

The flow rate at the northern most site, Waco, is largely controlled by water released from upstream reservoirs (Whitney, Aquilla, and Waco) and is only slightly impacted by local rainfall. A station upstream of Waco, USGS gage 08093100 near Aquilla, was used to gain some information about the amount of water being released from Whitney on its way to Waco; Whitney continually releases water since it is inline with the main stem of the Brazos. However, releases from lakes Aquilla and Waco also impact the flow rate at Waco. Releases from these two reservoirs are much more difficult to predict since they only release water if their conservation pool are exceeded. The dependence of the flow at Waco on the reservoir releases and the difficulty in predicting reservoir release rates and timings made predicting flow conditions at Waco challenging.

Downstream of Waco, flow rates were easier to predict using the amount of water passing the Waco station from reservoir releases and the rain amounts and locations over the lower Brazos watershed (downstream of the reservoirs). To estimate the response of the lower watershed to rainfall, recorded rainfall patterns and discharge hydrograph at the five lower gages were analyzed for a three day rain event that took place over the lower watershed from January 15-17, 2011, with 0.02, 0.27 and 0.36 inches of rain falling on each day respectively. During the event, rain fell over the entire lower Brazos watershed but was more strongly concentrated in the regions surrounding the Waco and Highbank gages. Figure 3.1 shows the hydrograph for each of the different gages in response to the event. The approximate travel time of the flood wave between the gages for the event is given below Table 3.3.

While the exact time it takes for a flood wave to pass from one gaging site to another

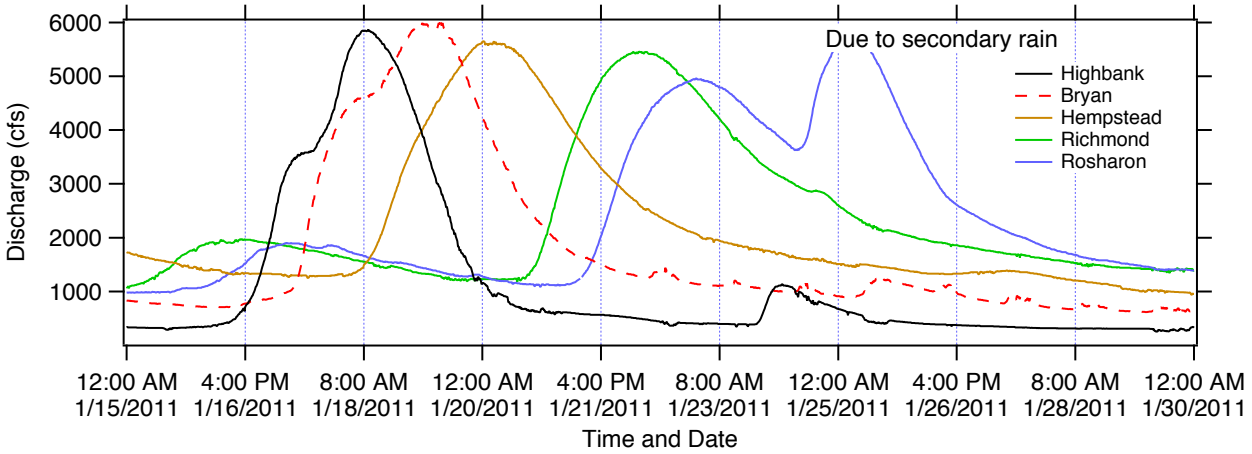

Figure 3.1: Discharge time series at the five lower gaging stations in response to the rain event over Lower Brazos River watershed on January 15, 16, and 17 of 2011.

From	To	Approximate Travel Time
Highbank	Bryan	22 hrs
Bryan	Hempstead	22 hrs
Hempstead	Richmond	49 hrs
Richmond	Rosharon	18 hrs

Table 3.3: Approximate travel times between the lower five gage sites.

change as a function of rain fall location and intensity, the values obtained from this analysis did provide some helpful guidelines about the timing and attenuation of the flood wave as it passed through the system. This information, along with daily monitoring of the flow rates at the USGS gage stations and monitoring of the National Weather Service predicted and measured rainfall over the lower watershed was used to plan sampling trips.

3.4 Data collection methods

All six of the gage sites are located at bridge crossing (fig. 1.2, 1.3). Accessibility to the bridge decks for sampling purposes varies with location. The Richmond bridge has a pedestrian walkway running from one side to the other (fig. 3.2A). This makes data collection from the bridge quite easy since no lane or shoulder closure is needed. Waco, Bryan, and Hempstead all have shoulders across the bridge and require closure of the shoulder for safety when making measurements (e.g., fig. 3.2B). The Highbank and Rosharon sites both lack any shoulder over the bridge and require a full lane closure if data is to be collected from the bridge (e.g., fig. 3.2C). The company N-LINE Traffic Maintenance was used for all sites needing lane closures. For sites that only needed shoulder closures, the appropriate signs, barricades, and cones were used to protect field personnel following Traffic Control Plans (TCP) (1-1b)-98 as specified by the Texas Department of Transportation.

The primary data collected during each sampling trip included: a cross-sectionally integrated water column sample for measurement of the suspended sediment concentration, a

Figure 3.2: Examples of different shoulder conditions across the bridge deck. (A) the Richmond bridge with a pedestrian walkway; (B) the Bryan bridge with a shoulder closure; and (C) the Highbank bridge with now shoulder.

cross sectionally integrated water column sample for measurement of the grain size distribution of the material in suspension, a bed material sample for characterization of the bed material size distribution, and measurement of the river boundary at the cross section.

The water column samples used for determination of the suspended sediment concentration and grain size distribution were obtained using a Federal Interagency Sedimentation Project (FISP) depth-integrated sampler (US DH-2TM bag-type) and the Equivalent Width Increment (EWI) method (Diplas et al., 2008). The US DH-2TM bag-type sampler is designed to collect 1 L isokinetic samples in depths up to 35 ft and velocities in the range of 2.0 to 6.0 ft/sec. The sampler was lowered and raised using a three-wheel truck USGS Type A crane with a B-56M sounding reel (fig. 3.3A). Nozzles of differing inner diameter (3/16", 1/4", and 5/16") were used to optimize the sampler for the flow conditions present at the time of sample collection, while keeping the sampler transit rate through the vertical limited to 40% of the mean channel velocity (Edwards and Glysson, 1999; Davis, 2005). All water samples from individual vertical transits were combined to create a integrated samples for the cross section following the EWI method. In general, velocities on the Brazos were too slow during the "low" flow conditions for use of the depth-integrated sampler. When deployed during these periods of low velocity, the sampler simply would not fill with water. Therefore, for the low flow conditions, a rope was tied to a bucket which was then lowered into the river and raised to obtain water column samples for the low flow conditions. During bucket sampling, the bucket remained close to the free surface due to buoyancy.

Figure 3.3: Primary sampling equipment. (A) US DH-2TM bag-type sampler suspended from the sampling crane; (B) US BMH-60 bed material sampler; and (C) sounding weight.

A US BMH-60 FISP scoop-type bed material sampler suspended from the sampling crane (fig. 3.3B) was used to collect samples of the bed material at each measurement increment across the channel width. All samples were combined in a bucket to provide a single representative bed material sample for the cross section. Cross sectional data was obtained using a sounding weight dropped from the bridge deck using the sampling crane (fig. 3.3C). At each increment across the width, the distance to the bed and water surface from the bridge railing was recored. For consistency, the sampling increments across the bridge were setup from the same starting point on each repeated visit. During most of the high flow conditions, drag on the sounding weight and bed material sampler as they passed down through the water column was great enough to prevent data from being obtained with the sounding weight and bed material sampler.

Field samples of suspended sediment were processed in the laboratory to obtain average the suspended sediment concentration, C, associated with each particular flow discharge. Measurements of the total suspended sediment concentration was obtained through filtering of the sample following the ASTM standards outlined in ASTM D3977 - 97(2007) (ASTM, 2007). Bed material samples were sieved to produce a percent finer than by weight grain size distribution. The grain size distribution of the sediment in suspension was measured by running small, well-mixed water column samplers through a Malvern Mastersizer capable of measuring particle sizes in the range of 0.05 μm to 0.9 mm.

4 Data

4.1 Summary of flow conditions captured

This project officially ran from August 1, 2010 to August 30, 2012. However, all of the moderate and high flow samples were collected between October 2011 and July 2012 due to lack of sustained rain from the start of the project up and through December, 2011. In total, 33 of the planned 36 measurements were made. Two moderate flow conditions at Waco and one at Highbank were not captured during the study time window. This is due in part to the difficultly in predicting the flows at these two stations with enough lead time to mobilize the field sampling equipment and crew, and also due in part to the limited amount of time the Brazos was between the 50 and 90% exceedance values during the study.

The largest flow event to occur during the sampling period took place during the last week of March 2012. During this event, flows at each of the stations reached or slightly exceeded the 2-year return period flow (table 3.2). Suspsended sediment measurements were captured during the peak of this event for Hempstead, Richmond, and Rosharon. Measurements made at the three most upstream stations were made on the falling limb of this event.

4.2 Notes on measured data

Summary figures of the collected data are shown below figures 4.1-4.6, and all collected data is listed in table 4.1. Discharges shown in the figures and tables are the 15-minute USGS instantaneous discharges. The actual discharge at the time of measurement was typically slightly different than the mean daily value. However, we use the mean daily discharge throughout since the effective discharge calculations are based on mean daily data.

Two types of concentrations and suspended sediment discharges are reported. The first is the total suspended sediment load, Q_{ss} [tons/day], which contains both suspended bed material and suspended wash load; suspended bed material was defined as material coarser than 0.062 mm. Q_{ss} is calculated using the total concentration measurement from the sampler multiplied by the volume of flow passing the station in one day,

$$Q_{ss} = (1.1 \times 10^{-6}) C_{ss} V_{24\text{hr}} \tag{4.1}$$

where C_{ss} is the concentration in g/m^3 (which is equivalent to the concentration in mg/l), $V_{24\text{hr}}$ is the volume of water in m^3 passing the station per day, and 1.1×10^{-6} is a factor used to convert from grams to US short tons so that the units on Q_{ss} work out to be tons/day. The second type of suspended sediment load shown in the figures and tables and used in the analysis is the suspended bed material load, Q_{sbm}, computed as,

$$Q_{sbm} = \left(\frac{100 - \%WL}{100} \right) Q_{ss} \tag{4.2}$$

where, $\%WL$ is the wash load percentage, defined as the percent by volume of the material traveling in suspension that is less than 0.062 mm. $\%WL$ was calculated using the Malvern

measured suspended sediment grain size distributions. For sampling dates without Malvern measurements of the suspended sediment, $\%WL$ values for flows that most closely matched the missing data were used (table 4.1). As will be discussed in the next section, the percent wash load used in the development of the rating curves for some sampling data was modified so that the developed rating curves for suspended bed material load have reasonable slopes with the calculated suspended bed material load being less than the total load in suspension (wash load + suspended load) over the entire range of the discharges used in the analysis.

In general, suspended sediment discharge increased with stream discharge. However, measured within stream concentrations of combined suspended bed material and wash load during the first large flow event sampled tended to be larger than those sampled during the second high flow event, even though the discharge during the second event often exceeded that of the first. This trend of a larger sediment discharge during the first lower increase in discharge occurred in our data set for Waco, Bryan, Hempstead, Richmond, and Rosharon. Maximum observed suspended sediment concentrations per site are marked in table 4.1 with bold text, and the maximum daily discharge during the sampling at each site is highlighted with italics. Bolded italics are used when the two maximums coincide. This occurred only for for the Highbank dataset, and a following discharge very close to the maximum but again resulted in a much reduced measured concentration (table 4.1). The overall maximum observed total suspended sediment concentration occurred at Hempstead during the first increase in flow after the 2011 drought. During this event, concentrations reached C_{ss} = 6.9 g/l though discharge was only a modest 16,000 cfs (figure 4.4). A suspended material sample was not collected for particle sizing during this event, so a wash load percentage of 97% was assigned to the sample based on later measurement of the size distribution during a similar flow event.

An unusual trend present in the dataset for both the suspended sediment and bed material, is that grain size in each tends to fine with increasing discharge. While the trend is not completely consistent in that size is inversely related to discharge, suspended sediment samples taken during the high flow conditions did consistently produce some of the finest observed suspended sediment grain size distributions (figures 4.1-4.6). This trend was not as prominent in the bed material samples, though samples from Hempstead were coarsest during the low flow conditions (figure 4.4).

Channel geometry sections are expected to be the most accurate during the low flow conditions. During high flow, it is possible that drag on the sounding weight made the cross section appear to be "deeper" than it actually was due to the angled line of fall of the weight (e.g., figures 4.1, 4.2); however, this trend was not consistent throughout (figure 4.6). Furthermore, it is possible that changing thicknesses of the vegetation throughout the year may have also impacted the soundings on the banks, leading to some of the large deviations in measured cross sectional form (figure 4.2, 4.5).

Figure 4.7 shows some of the downstream trends for drainage area, slope (discussed in detail in the next section), active channel width, bankfull depth, return period flows at 1.5, 2, and 10 years, and the average bed material grain size statistics. An item of note from these plots is the Hempstead tends to have the largest discharge statistics, the smallest slope, and the finest bed material. Another item of interest is that from Waco to Richmond, the unobstructed width of the channel stays fairly constant to slightly increasing, but then decreases from Richmond to Rosharon. This trend mirrors the $Q_{1.5}$ trend, but not the Q_2 or Q_{10} trends. Channel depth on the other hand continually increases downstream.

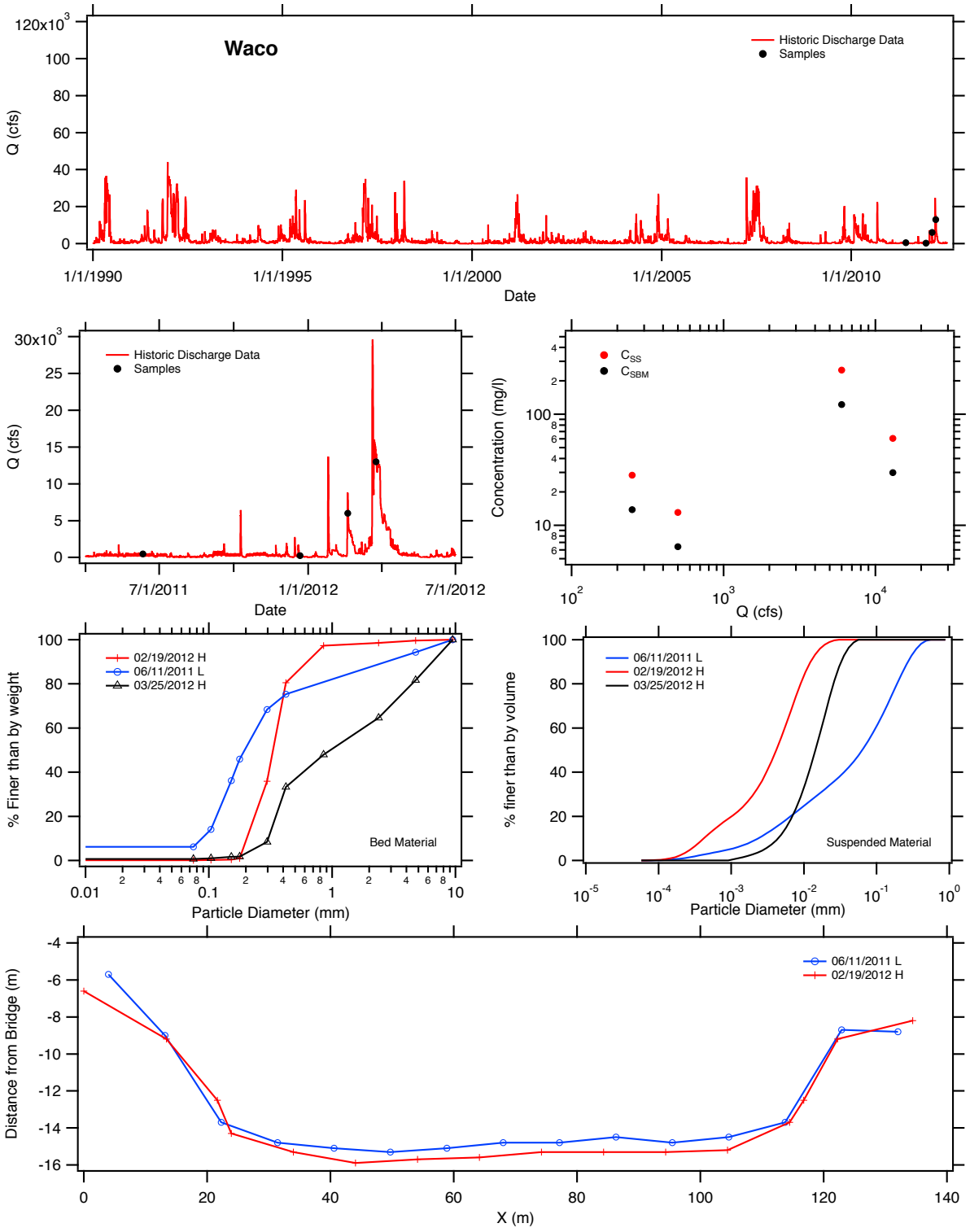

Figure 4.1: Summary of collected data at Waco (USGS gage 0809650).

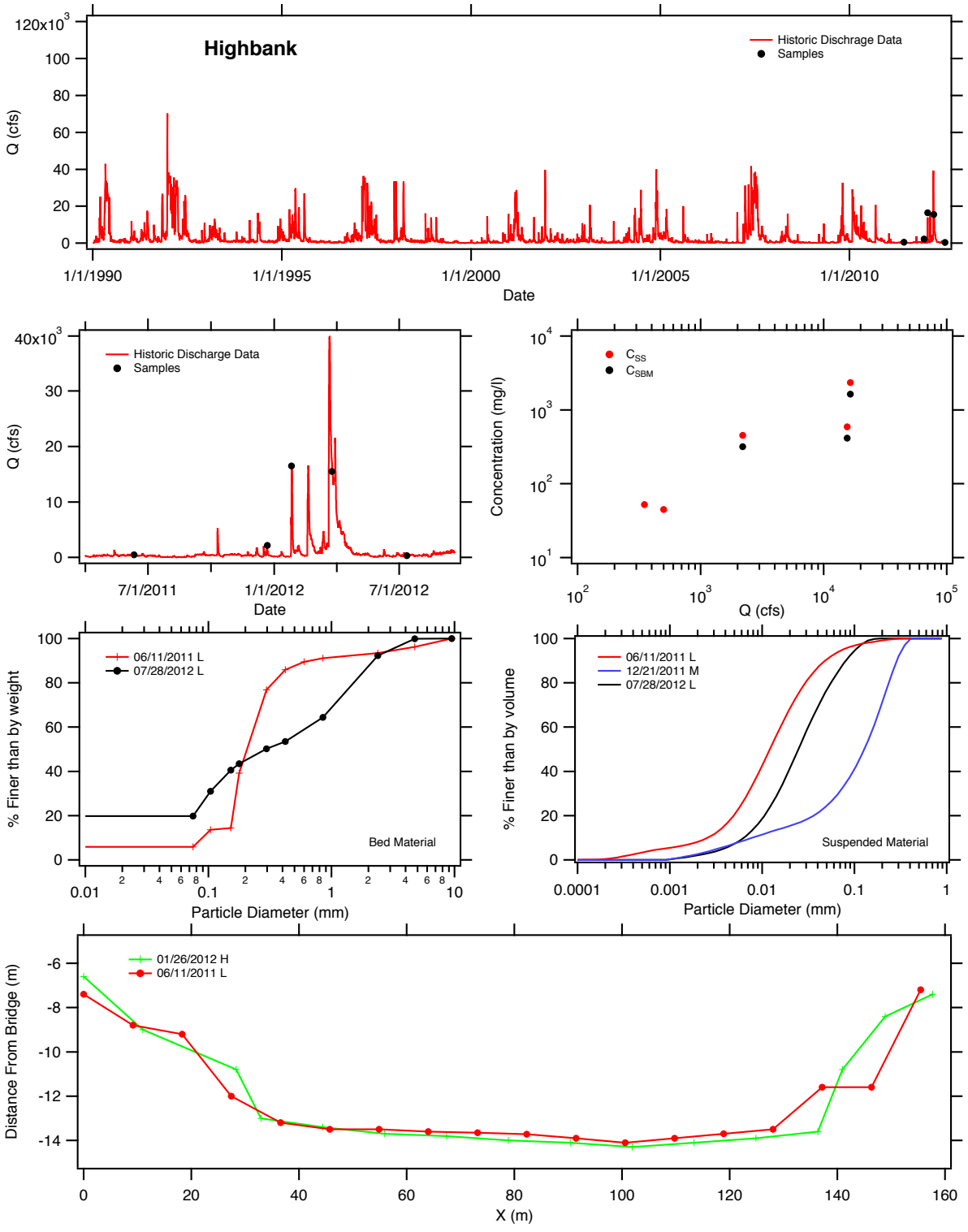

Figure 4.2: Summary of collected data at Highbank (USGS gage 08098290).

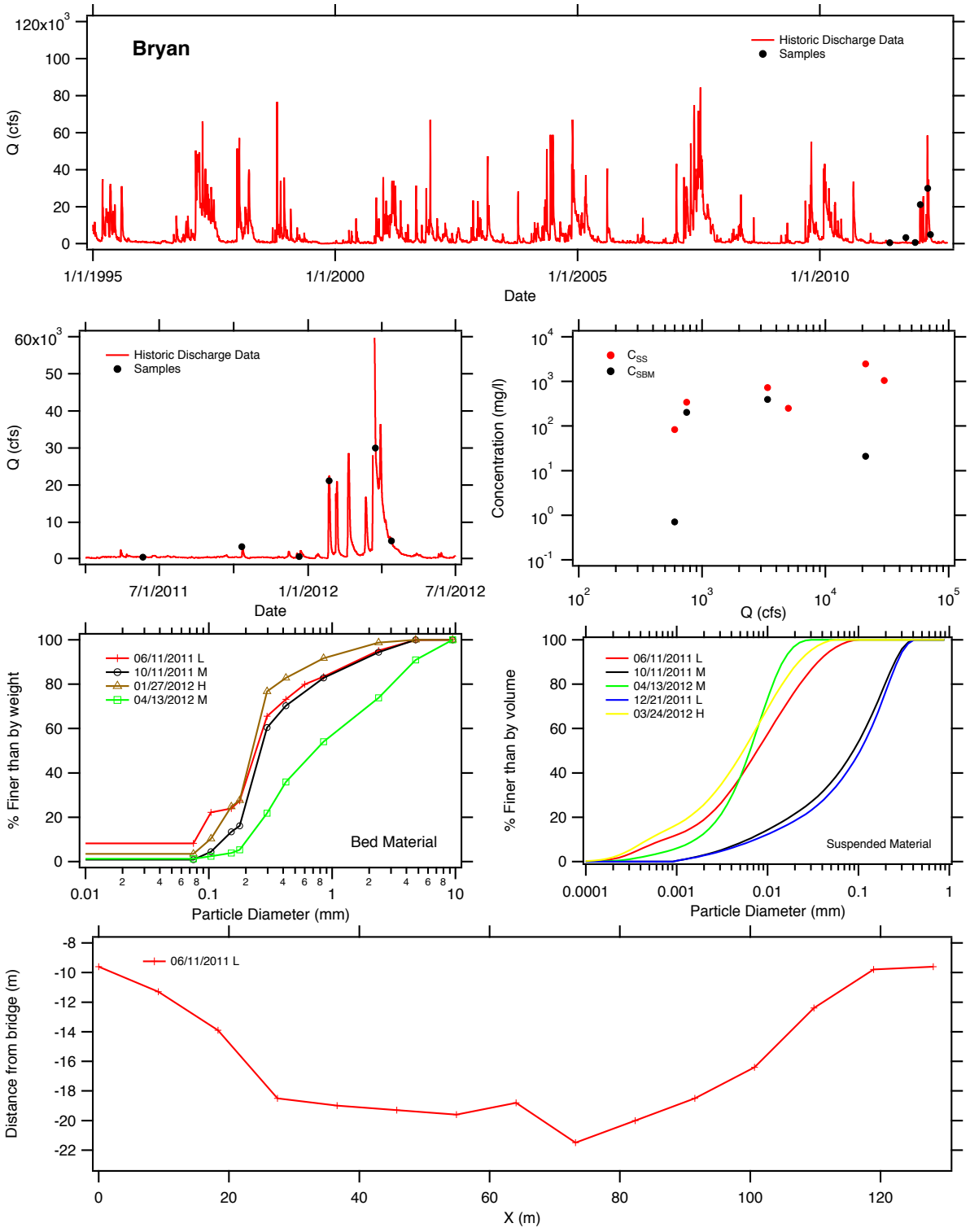

Figure 4.3: Summary of collected data at Bryan (USGS gage 08108700).

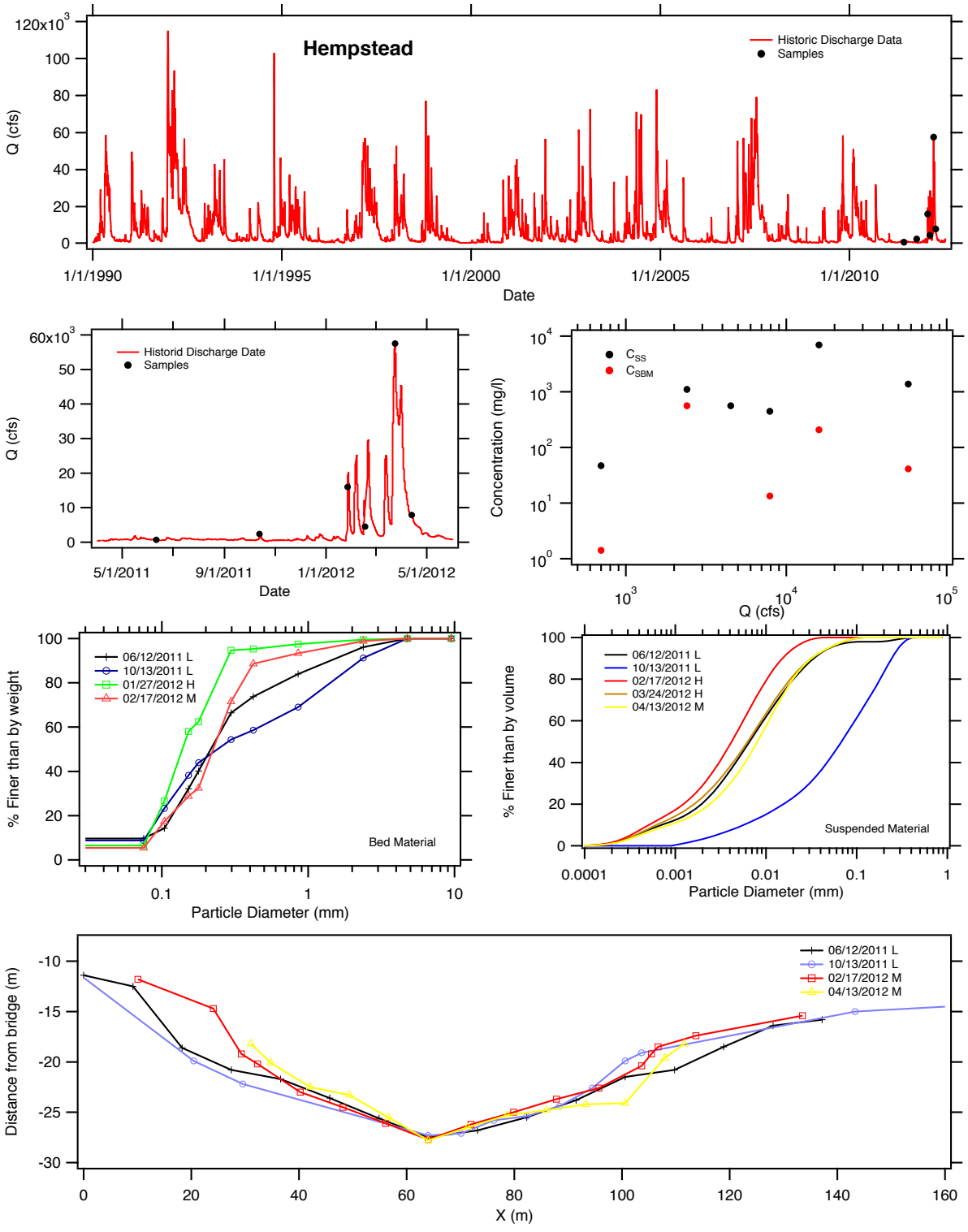

Figure 4.4: Summary of collected data at Hempstead (USGS gage 08111500).

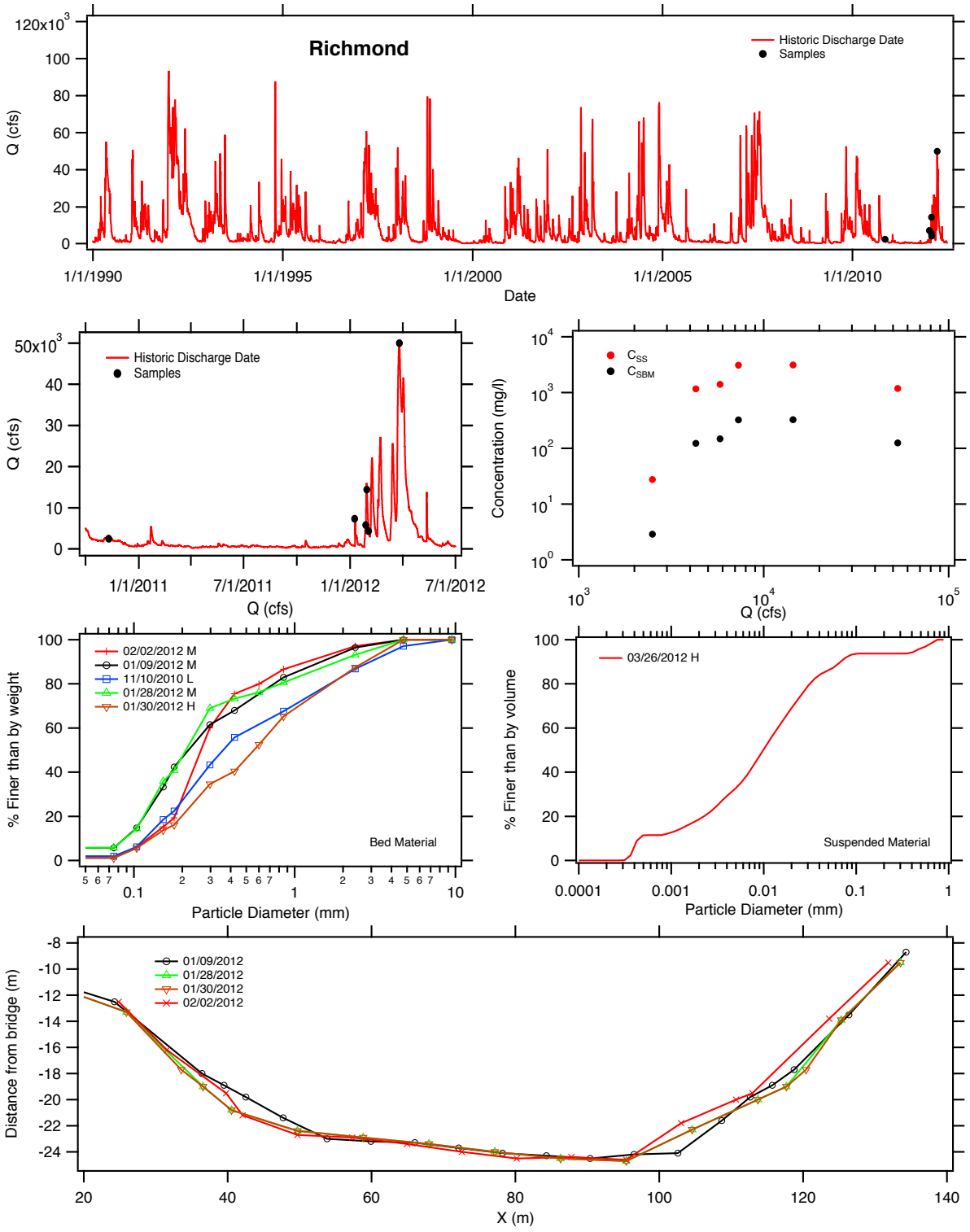

Figure 4.5: Summary of collected data at Richmond (USGS gage 08114000).

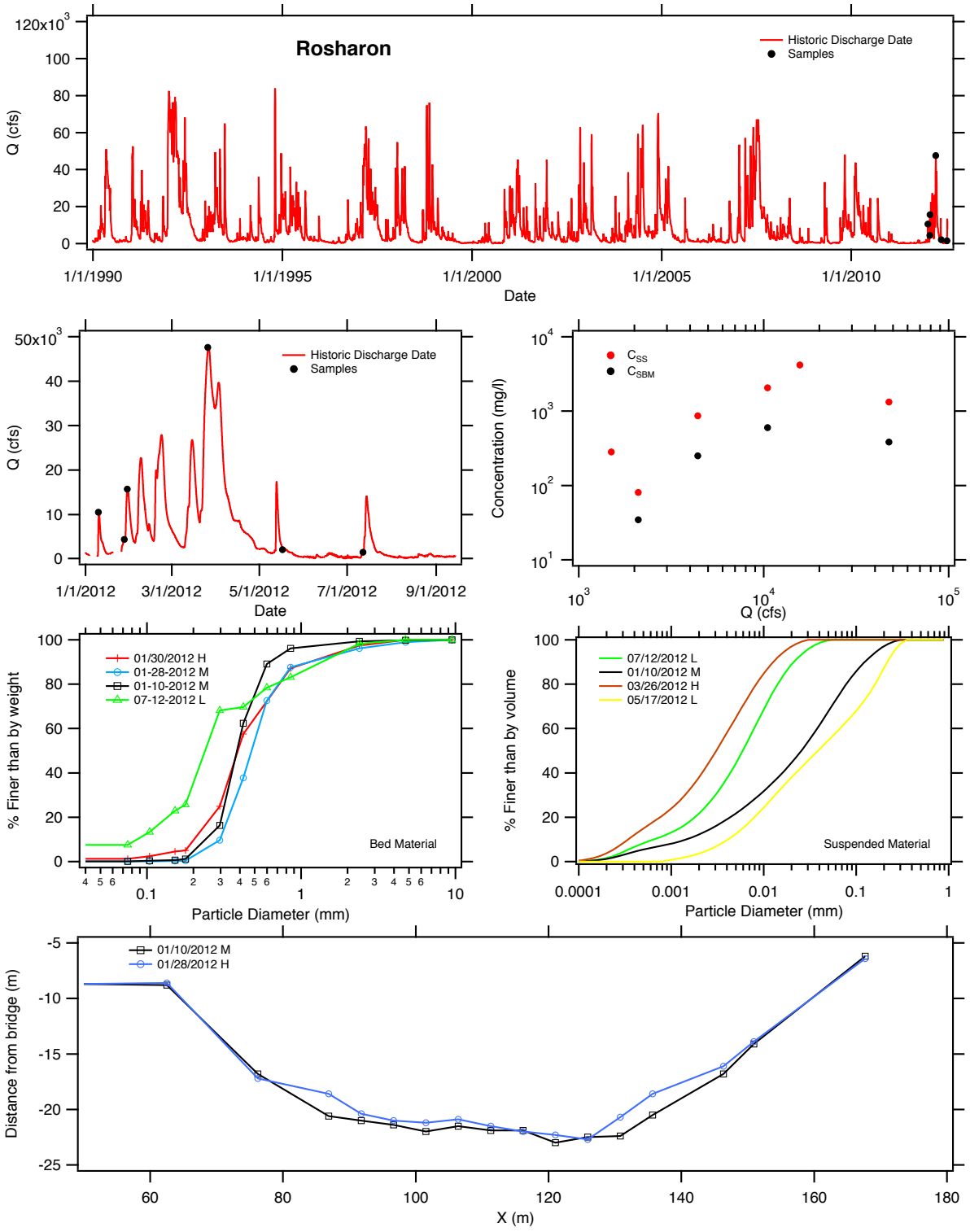

Figure 4.6: Summary of collected data at Rosharon (USGS gage 08116650).

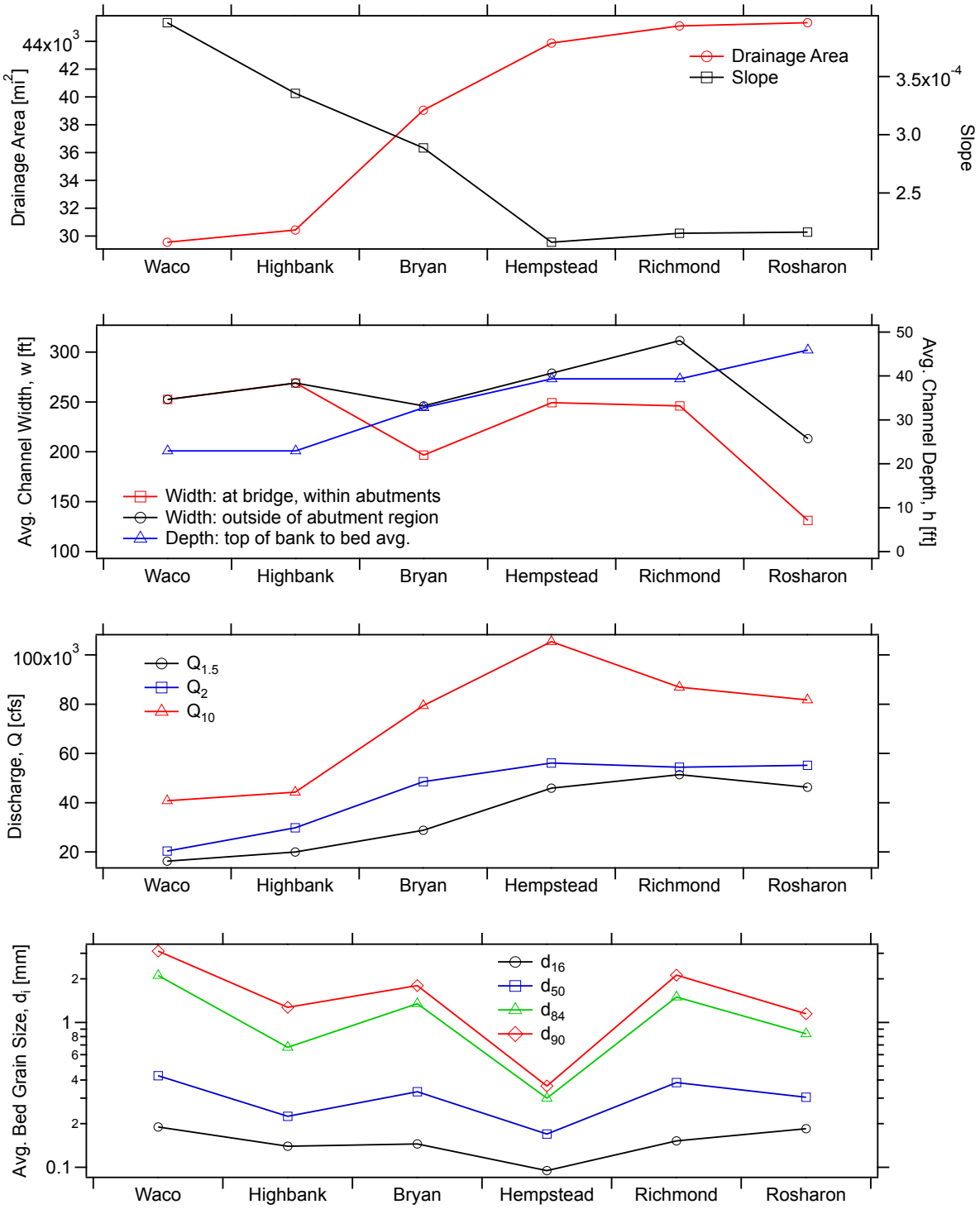

Figure 4.7: Downstream trends in major steam properties.

Site	Date	Condition	Location on Hydrograph	SS Sample Method	Bed Size Measured? (Used)	SS Size Measured? (Used)	Q [cfs]	R_h [ft]	U [ft/s]	Bed Material d_{16} [mm]	d_{50} [mm]	d_{84} [mm]	d_{90} [mm]	Wash Load [%]	Total SSC [mg/l]
Waco	06/11/11	Low	Base	Bucket	Yes	Yes	500	3.4	0.5	0.11	0.20	1.50	2.70	51	13
Waco	12/22/11	Low	Base	Bucket	No (6/11/11)	No (6/11/11)	250	3.0	0.3	0.11	0.20	1.50	2.70	51	28
Waco	02/19/12	High	Falling	DIS	Yes	Yes	**6,000**	8.8	2.2	0.22	0.32	0.45	0.55	51*	**250**
Waco	03/25/12	High	Falling	DIS	Yes	Yes	*13,000*	13.4	2.8	0.32	1.00	5.00	6.50	51*	*61*
Highbank	06/11/11	Low	Base	Bucket	Yes	Yes	500	0.8	2.5	0.16	0.20	0.40	1.00	100*	45
Highbank	12/21/11	Moderate	Peak	DIS	No (6/11/11)	Yes	2,200	2.0	4.1	0.16	0.20	0.40	1.00	30	452
Highbank	01/26/12	High	Peak	DIS	No (6/11/11)	No (12/21/11)	***16,500***	8.6	4.7	0.16	0.20	0.40	1.00	30	***2,339***
Highbank	03/25/12	High	Falling	DIS	No (6/11/11)	No (12/21/11)	15,500	7.7	4.9	0.16	0.20	0.40	1.00	30	591
Highbank	07/28/12	Low	Base	Bucket	Yes	Yes	350	0.8	1.7	0.08	0.30	1.50	2.10	100*	52
Bryan	06/11/11	Low	Base	Bucket	Yes	Yes	600	3.3	0.8	0.09	0.21	0.90	1.30	99	83
Bryan	10/11/11	Moderate	Peak	DIS	Yes	Yes	3,400	6.4	2.3	0.17	0.26	0.90	1.30	46	728
Bryan	12/21/11	Low	Base	Bucket	No (6/11/11)	Yes	750	3.3	1.1	0.09	0.21	0.90	1.30	41	342
Bryan	01/27/12	High	Peak	DIS	Yes	No (06/11/11)	**21,200**	17.6	3.0	0.12	0.21	0.50	0.70	99*	**2,475**
Bryan	03/24/12	High	Falling	DIS	No (1/27/12)	Yes	*30,000*	20.4	3.4	0.12	0.21	0.50	0.70	100	*1,044*
Bryan	04/13/12	Moderate	Falling	DIS	Yes	Yes	5,000	9.0	1.6	0.25	0.70	3.50	4.50	100	249
Hempstead	06/12/11	Low	Base	Bucket	Yes	Yes	700	10.6	0.2	0.11	0.21	0.85	1.20	97	47
Hempstead	10/13/11	Low	Peak	Bucket	Yes	Yes	2,400	14.3	0.6	0.09	0.22	1.80	2.30	49	1104
Hempstead	01/27/12	High	Rising	DIS	Yes	No (03/24/12)	**16,000**	21.5	1.8	0.09	0.13	0.25	0.28	97	**6,938**
Hempstead	02/17/12	Moderate	Rising	DIS	Yes	Yes	4,500	15.6	1.1	0.10	0.21	0.35	0.45	100	560
Hempstead	03/24/12	High	Peak	DIS	No (1/27/12)	Yes	*57,500*	27.2	2.1	0.09	0.13	0.25	0.28	97	*1,372*
Hempstead	04/13/12	Moderate	Falling	DIS	No (2/17/12)	Yes	7,900	17.9	1.6	0.10	0.21	0.35	0.45	97	446
Richmond	11/10/10	Low	Base	Bucket	Yes	No (3/26/12)	2,500	10.5	1.0	0.14	0.37	2.00	3.00	90	27
Richmond	01/09/12	Moderate	Peak	DIS	Yes	No (3/26/12)	7,300	12.9	2.2	0.11	0.22	0.86	1.60	90	3,092
Richmond	01/28/12	Moderate	Rising	DIS	Yes	No (3/26/12)	5,800	12.1	1.8	0.11	0.21	1.20	1.70	90	1,405
Richmond	01/30/12	High	Peak	DIS	Yes	No (3/26/12)	**14,400**	15.3	3.2	0.17	0.54	2.00	2.70	90	**3,117**
Richmond	02/02/12	Moderate	Falling	Bucket	Yes	No (3/26/12)	4,300	11.3	1.6	0.16	0.25	0.80	1.40	90	1,166
Richmond	03/26/12	High	Peak	DIS	No (1/30/12)	Yes	*53,000*	25.8	6.0	0.17	0.54	2.00	2.70	90	*1,187*
Rosharon	01/10/12	Moderate	Peak	DIS	yes	Yes	10,500	13.0	3.4	0.29	0.38	0.55	0.61	71	2,062
Rosharon	01/28/12	Moderate	Rising	DIS	yes	No (01/10/12)	4,400	8.1	3.1	0.31	0.46	0.72	1.00	71	863
Rosharon	01/30/12	High	Peak	DIS	yes	No	**15,700**	15.5	4.0	0.25	0.38	0.77	1.00	100	**4,185**
Rosharon	03/26/12	High	Peak	DIS	No (1/30/12)	Yes	*47,600*	27.3	5.7	0.25	0.38	0.77	1.00	71*	*1,325*
Rosharon	05/17/12	Low	Falling	Bucket	No (7/12/12)	Yes	2,100	6.6	1.9	0.12	0.23	0.90	1.30	57	81
Rosharon	07/12/12	Low	Rising	Bucket	yes	Yes	1,500	6.2	1.5	0.12	0.23	0.90	1.30	100	282

Table 4.1: Summary of measured data. **Bolded** text highlights the highest measured concentrations at that site, and the *italics* highlights the highest daily main discharge during the sampling at the site. For the ***bolded italics***, the two maximums coincided. *Wash load values used in the development of the sediment rating curves.

4.3 Comparison of data to historic sources

The collected suspended and bed material samples were compared to USGS measured values when available. Of the six sites, the USGS has recorded suspended sediment measurements for Highbank, Richmond, and Rosharon. No bed load data was found at any of the sites, and only the Richmond site contained bed material grain size data.

Of the three sites, the Richmond station has the largest volume of historic data. The USGS dataset for this site contains suspended sediment measurements from 1966 to 1995 along with three bed material samples from 1966. Sediment related data for the site can be obtained from the NWIS gage page or through the Suspended-Sediment Database [http://co.water.usgs.gov/sediment/seddatabase.cfm]. The number of total suspended concentrations and daily loads measurements at the Richmond site for this time period is 7553. However, only a subset of this database (229 measurements) contain corresponding data regarding the percentage of the total suspended material less than 0.0626 mm. The data for which the suspended sediment size information is available can be obtained through the ancillary data page, or from the main NWIS gage site. For this subset of data, the percent wash load can be determined from the percentage of material finer than 0.0625 mm and the suspended bed material load (or sand load) can be calculated using equation 4.2.

A time series of the USGS calculated suspended bed material load, Q_{sbm}, and discharges from are shown in figure 4.8. From simple observation of the plotted data, it appears that sand load at the Richmond station from 1984 to 1995 was reduced comparatively to loads prior to 1984 for similar discharges (figure 4.8). Since the time series is built from irregularly spaced discrete measurement, it is not possible to say if the overall sand load at Richmond was reduced from 1984 onward. However, the observations seem to suggest that there has been a reduction in the measured high magnitude sand load events.

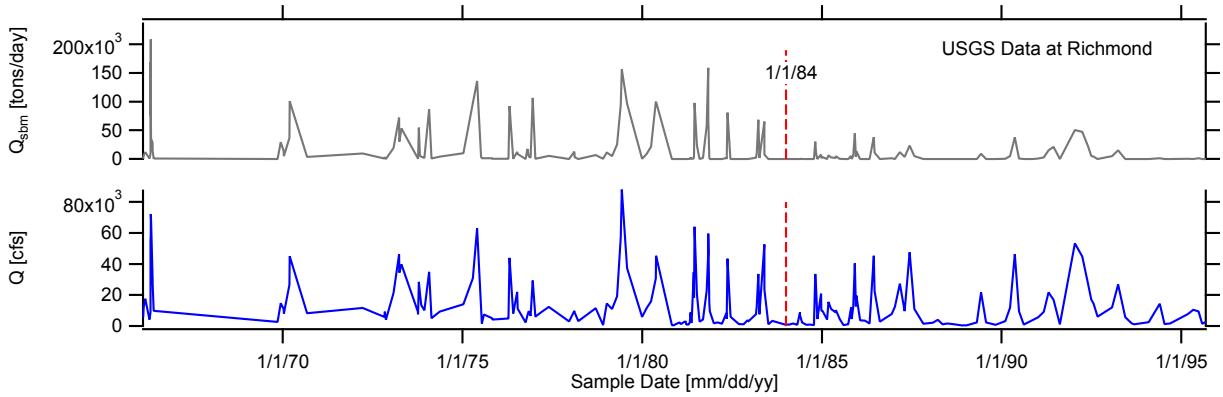

Figure 4.8: Measured sand load and discharge at the Richmond gage site. Data obtained from the USGS Suspended-Sediment Database.

Comparisons of the measured concentrations and suspended bed material load with the historic data shows that the newly measured concentrations and loads fall within the range of those previously observed but near the outskirts of the band typical historic values (figure 4.9A). The measured concentrations at the lowest and high discharges were less than those typically observed at similar discharges from 1966 to 1995. At the four moderate discharges, the measured concentrations were, on average, higher than the historic values (figure 4.9A). During our

sampling at Richmond, only one suspended sediment sample was analyzed for grain size. The analyzed sample was collected during the largest flow event sampled at the Richmond station during the peak of the hydrograph (Q = 53,000 cfs). The grain size analysis for this sample showed that 90% of the material in suspension was wash load. This again falls into the range of observed historic values, but is slightly larger than the average for flow given discharge (figure 4.9B).

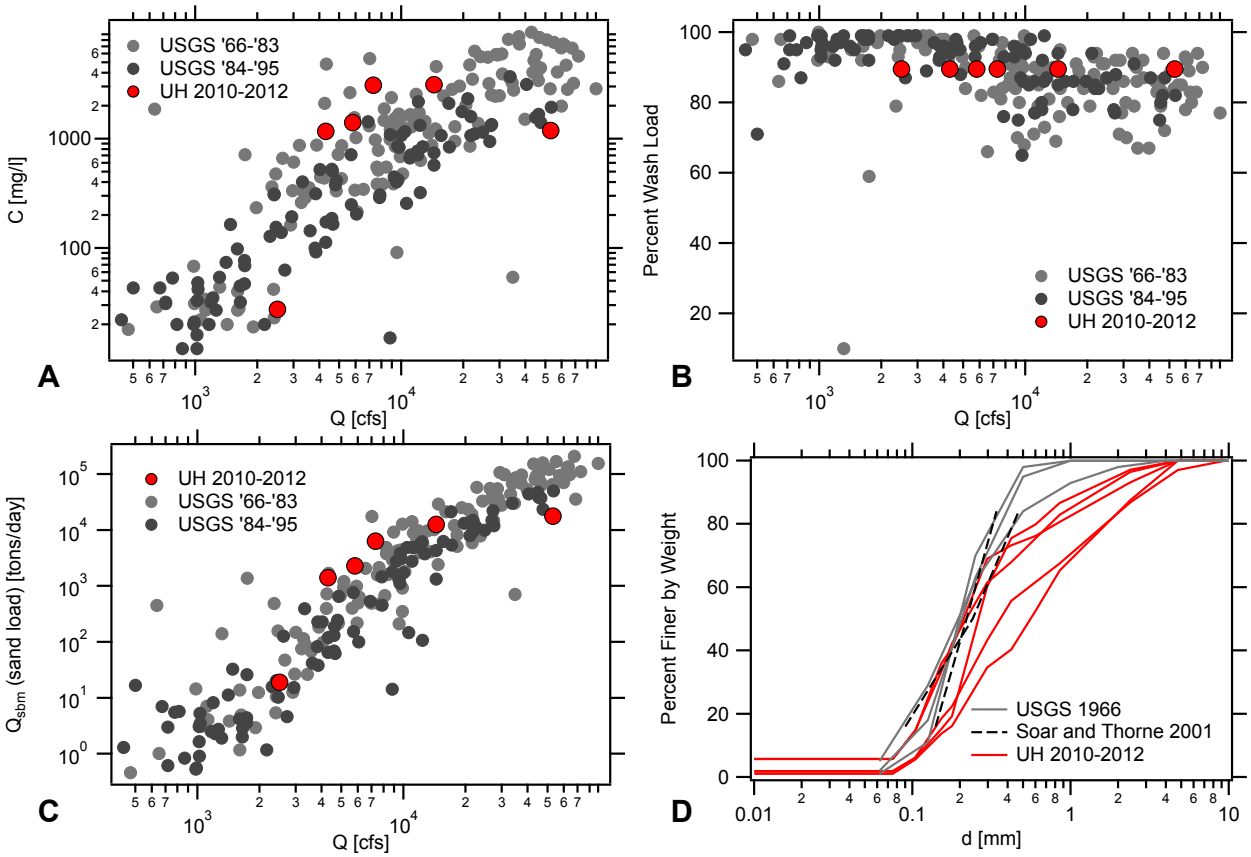

Figure 4.9: Comparison of UH and USGS data at the Richmond station.

Because only one suspended sediment sample was sized at Richmond, the 90% wash load value was applied uniformly for all suspended sediment samples collected at the site (figure 4.9B). The 90% value seems to be within a reasonable range for the moderate discharges relative to the historic data, but is on the lower end of observed values for the smallest discharge. The historic and current measured wash load percentages where used to calculate the suspended sand load (figure 4.9C). The scatter of measured and historic suspended sand loads as a function of discharge are similar to those of the overall total concentration. The loads at the largest discharge are small compared to the historic data while moderate discharges are within the range are slightly higher than the average tend of historic data.

The measured bed material grain size distributions were also compared to historic values (figure 4.9D). USGS data for the bed material grain size distribution at Richmond was limited to three samples from 1966. Two additional samples containing, d_{16}, d_{50}, and d_{84} size information were obtained from Soar and Thorne (2001) (Brazos sites A and B, data is listed in their Table

B3 of the appendix). The bed material samples taken during the moderate flow conditions of 1/09/12 and 1/28/12 best matched the historic USGS 1966 and the Soar and Thorne (2001) data (figures 4.5, 4.9D). The cumulative grain size distribution curves from these two samples match the historic data well from d_{16} through $\approx d_{60}$, but coarsen relative to the historic data from sizes greater than $\approx d_{60}$. The other measured samples are coarser than the historic data throughout the cumulative curve.

Data for Highbank and Rosharon was obtained from the NWIS sites for each gage under the "Water Quality: Field/Lab Sample" section. All suspended, bed, and bed material sediment data was checked for. No bed load or bed material data was found. For suspended sediment, the relevant data extracted were the total suspended sediment concentration (SSC) in mg/l (USGS key 80154), the suspended sediment discharge, Q_{ss} [tons/day] (USGS key 80155), and the percent of suspended sediment of diameter less than 0.0625 mm, i.e., the $WL\%$ (USGS key 70331). Data for these two sites can be found in figures 4.10 and 4.11

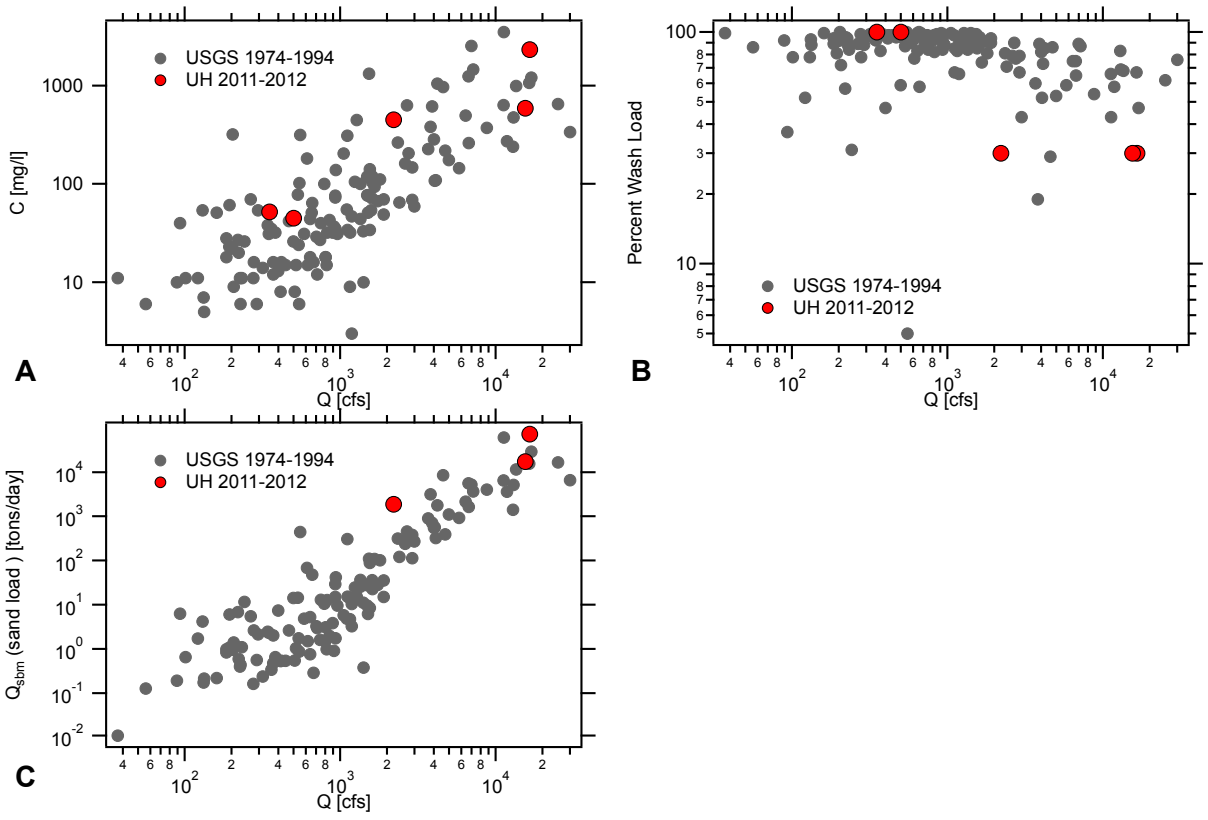

Figure 4.10: Comparison of UH and USGS data at the Highbank station.

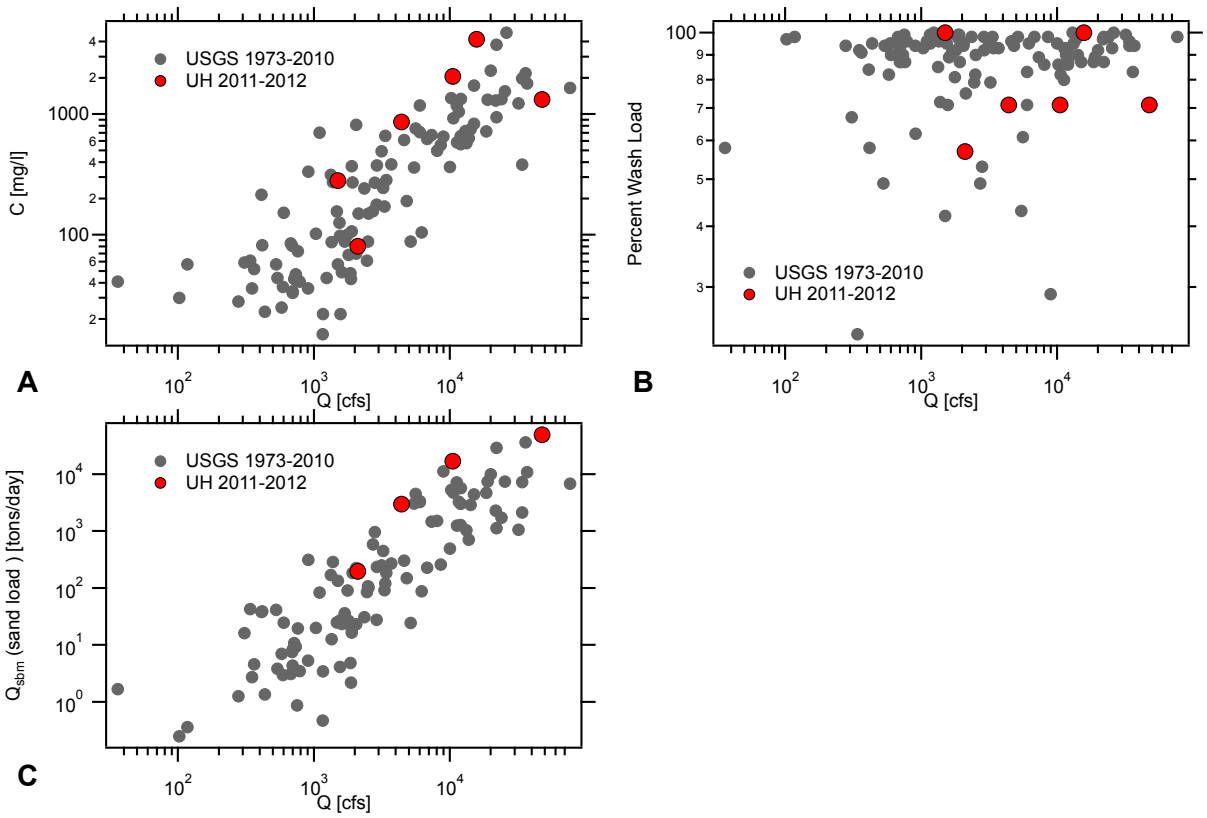

Figure 4.11: Comparison of UH and USGS data at the Rosharon station.

5 Analysis and Results

5.1 Sediment rating curves and transport calculations

Sediment rating curves for the suspended load, Q_{sbm}, and the bed load, Q_b, were developed and used to construct the sediment load histograms for the suspended load and bed load independently. The resulting histograms where then added together to produce the total bed material histograms from which the effective discharge was obtained. Sediment rating curves for the total sediment load traveling in suspension (wash load plus suspended bed material load) were also developed. The curves and calculations of effective discharge and annual sediment load associated with the inclusion of the wash load are given in appendix A. All rating curves retain the power-law functionality of equation 2.3. A list of all coefficients and the correlation coefficient for curve are listed in Table 5.1.

The suspended sediment rating curves for Q_{sbm} and Q_{ss} were developed using regression and the measured data (figure 5.1). The bed load rating curves were developed from regression by calculating the total bed load in tons per day associated with the daily discharge data at the time of sampling at each site. This produced curves that estimated the bed load in tons/day as a function of mean daily discharge. To calculate the bed load, the Einstein-Brown equation was used. The Einstein-Brown equation uses the original dimensionless parameters defined by Einstein (1942) with the two-part power-law curves of Brown (1950):

$$q_b^* = \begin{cases} 40F(\tau^*)^3 & \text{for } \tau^* \geq 0.182 \\ 2.15Fe^{-0.391/\tau^*} & \text{for } \tau^* < 0.182 \end{cases} \tag{5.1}$$

Here, q_b^* and τ^* are the dimensionless bed load transport rate and dimensionless bed shear stress respectively:

$$q_b^* = \frac{q_{bv}}{\sqrt{R_s g d_{50}^3}}, \quad \tau^* = \frac{\tau_B}{R_s \gamma d_{50}} \tag{5.2}$$

In these definitions, q_{bv} is volumetric bed load transport rate per unit width, τ_B is the bed shear stress, $R_s = (\rho_s - \rho)/\rho$ is the submerged specific gravity, and d_{50} is the sediment size for which 50% of the material is finer than by weight. F in equation 5.1 is the Rubey (1933) settling velocity factor:

$$F = \left[\frac{2}{3} + \frac{36\nu^2}{g d^3 R_s}\right]^{1/2} - \left[\frac{36\nu^2}{g d^3 R_s}\right]^{1/2} \tag{5.3}$$

In the Einstein-Brown equation, the stress driving transport is the stress associated with only the skin friction component of stress. Hence, $\tau_B = \tau'_B$ with,

$$\tau'_B = \gamma R' S = \rho u_*'^2 \tag{5.4}$$

where u'_* is the friction velocity associated with the skin friction and R' is the hydraulic radius associated with skin friction. In this framework, the total hydraulic radius is a summation of

the skin and form roughness associated hydraulic radii, $R = R' + R''$ were R'' is due to form roughness. The transport equation is solved using the Einstein skin friction resistance relation:

$$\frac{U}{u'_*} = 7.66\left(\frac{R'}{d_{65}}\right)^{1/6} \tag{5.5}$$

The depth and geometric properties of the cross section were measured at each site at the time of sampling. Therefore, if S is known and uniform flow is assumed (i.e., eq. 5.4 is valid), then R' and τ'_B can be calculated using equations 5.4 and 5.5 with U defined from continuity. However, no measurement of the channel or water surface slope were made. Slope measurements were not made at the time of sampling because the surveying equipment available to us (construction level and tape) was not accurate enough to measure the very small slopes on the Brazos. For this reason, values of S were obtained for all sites from a USGS database of computed slopes for Texas gaging stations rather than through on-site measurement.

The USGS computed slope used in the stress calculations for bed load (equation 5.4) is referred to as the "main-channel slope" (Asquith and Slade, 1997). The main-channel slope, S in our analysis, is defined as the change in elevation between the two end points of the main-channel divided by the distance, L (Asquith and Slade, 1997). In the calculation method, L is defined as the longest defined channel shown in a 10-meter digital elevation model (DEM) from the approximate watershed headwaters to the point of interest, and the elevation change between the two points is extracted directly from the 10-meter DEM. The main-channel slope is therefore more of a watershed slope based on the channel network than it is a local reach slope. Because of its calculation method, we suspect that the main channel slope values will be, on average, higher than the local reach slopes at the stations because the main channel slope by definition incorporate elevation change further up in the watershed where slopes are likely higher. Slopes values for each of the stations using these calculated slopes are: Waco S = 0.0004, Highbank S = 0.0003, Bryan S = 0.0003, Hempstead S = 0.0002, Richmond S = 0.0002, Rosharon S = 0.0002. Because of the way these slopes have been defined, they are likely to slightly over estimate the actually channel slope at the station if there is a relatively smooth continuous change in slope from the headwaters down to the point of interest. Calculation of bed load was also done using the so-called 10-85 slope, i.e., the slope of the main-channel from 10 percent up the channel from the station to the point at which 85 percent of the total channel length is reached. The differences between the main channel slope and the 10-85 slope were small enough that the ultimate effective discharge calculations were independent of the slope chosen.

A summary of all measured and calculated sediment loads used in development of the rating curves is given in Table 5.2. The table also lists the total calculated sediment loads of

$$Q_{tl} = Q_{sbm} + Q_b \tag{5.6}$$

which includes the bed load and the suspended load;

$$Q_{\text{sed-all}} = Q_{ss} + Q_b \tag{5.7}$$

which includes bed load, suspended load, and wash load; and the SAMwin derived total bed material load Q_{tl}. The SAMwin derived Q_{tl} was developed using the measured cross sectional

data and the computer program SAMwin, a Windows version of the SAM Hydraulic Design Package For Channels. The Engelund and Hansen total load equation (Engelund and Hansen, 1967) was used for calculating the total loads with SAMwin.

Of note from the calculations of total bed material load is that suspended load is much more significant than bed load in terms of total mass moved. Additionally, Q_{tl} based on the measured suspended and calculated bed load is of the same order of magnitude as the Q_{tl} calculated with SAMwin, though no general trends in the difference between the two were observed.

	Q_{sbm} [tons/day]			Q_{ss} [tons/day]			Q_b [tons/day]			Q_{SAM} [tons/day]		
Site	α	β	R^2	α	β	R^2	α	β	R^2	α	β	R^2
Waco	0.002	1.475	0.91	0.004	1.474	0.91	1e-04	1.565	0.97	6e-04	1.774	0.99
Highbank	0.018	1.498	0.87	0.001	1.866	0.97	0.208	1.028	0.92	0.010	1.550	0.99
Highbank (USGS)*	4e-06	2.208	0.81	4e-04	1.863	0.88						
Bryan	0.004	1.404	0.40	0.009	1.600	0.94	5e-05	1.616	0.91	0.002	1.621	0.99
Hempstead	0.001	1.509	0.59	0.002	1.778	0.85	3e-06	1.924	0.82	0.001	1.623	0.98
Richmond	1e-04	1.855	0.63	0.001	1.851	0.63	1e-09	2.745	0.96	5e-04	1.745	0.99
Richmond (USGS)*	7e-08	2.592	0.87	4e-05	2.165	0.90						
Rosharon	0.001	1.680	0.87	0.001	1.824	0.86	1e-04	1.596	0.99	0.004	1.561	0.99
Rosharon (USGS)*	2e-04	1.723	0.76	0.002	1.737	0.92						

Table 5.1: Rating curve coefficient values and correlation coefficients. *Rating curves developed using all of the historic USGS data at the site along with the additional data collected by UH.

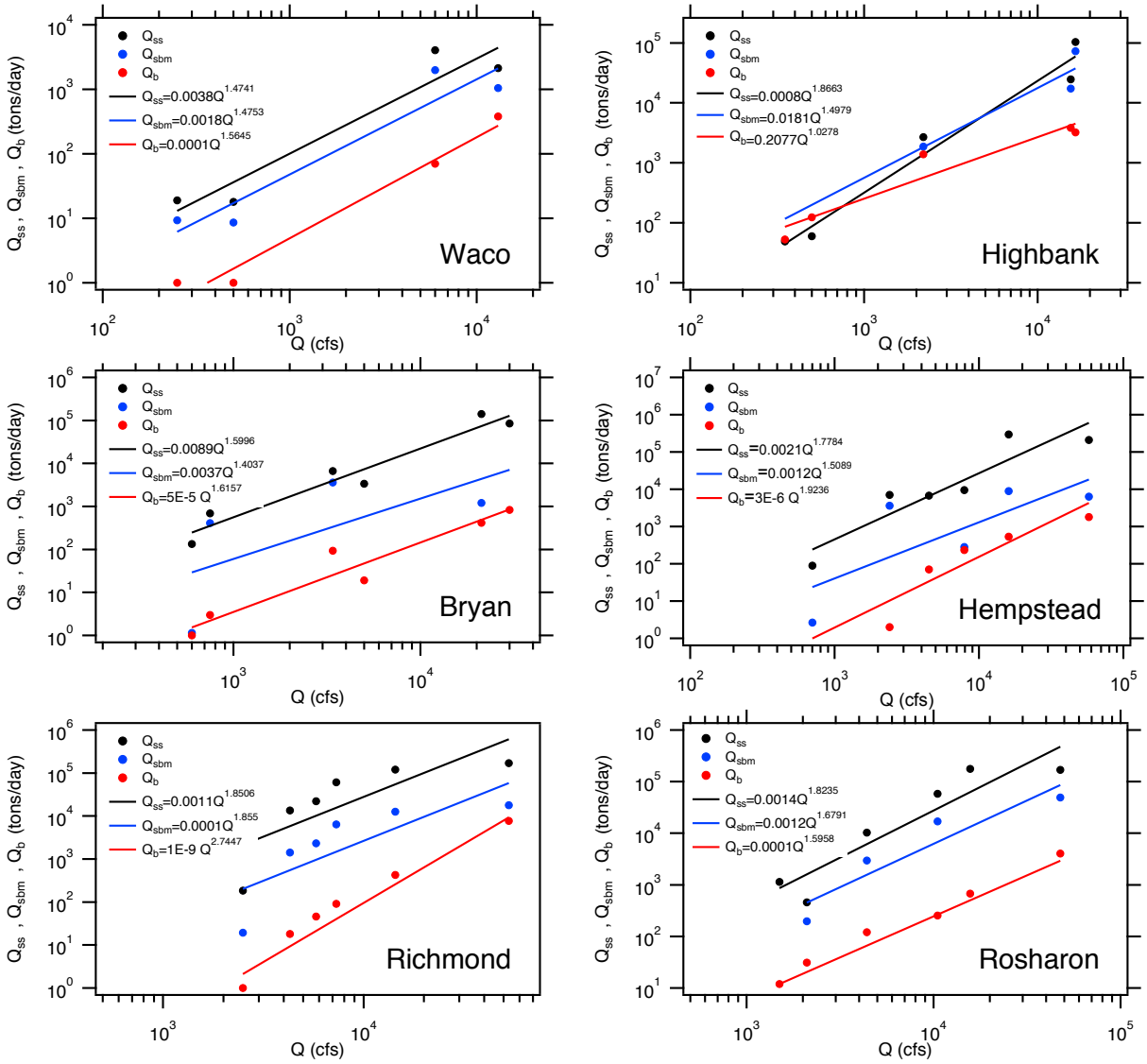

Figure 5.1: Rating curves.

Site	Date	Condition	S	Q [cfs]	d_{50} [mm]	τ^*/τ^*_{cr}	z_*	Trans. Mode[1]	Bedload Equation	Q_{ss} [T/day]	Wash Load [%]	Q_{sbm} [T/day]	Q_b [T/day]	$Q_{\text{sed-all}}$ [T/day]	Q_{tl} [T/day]	SAM Q_{tl} [T/day]
Waco	06/11/11	Low	0.0004	500	0.20	26	0.5	FS	Einstein-Brown	18	51	9	1	19	10	34
Waco	12/22/11	Low	0.0004	250	0.20	23	0.5	FS	Einstein-Brown	19	51	9	1	20	10	12
Waco	02/19/12	High	0.0004	6,000	0.32	53	0.6	FS	Einstein-Brown	4,034	51*	1,977	70	4,104	2,046	3,450
Waco	03/25/12	High	0.0004	13,000	1.00	22	1.3	T	Einstein-Brown	2,126	51*	1,042	381	2,507	1,422	11,807
Highbank	06/11/11	Low	0.0003	500	0.20	4	1.0	T	Einstein-Brown	60	100*	0	124	184	124	136
Highbank	12/21/11	Moderate	0.0003	2,200	0.20	13	0.6	FS	Einstein-Brown	2,677	30	1,874	1,394	4,071	3,268	2,088
Highbank	01/26/12	High	0.0003	16,500	0.20	85	0.3	FS	Einstein-Brown	103,870	30	72,709	3,222	107,091	75,931	30,852
Highbank	03/25/12	High	0.0003	15,500	0.20	68	0.3	FS	Einstein-Brown	24,669	30	17,268	3,812	28,481	21,080	28,629
Highbank	07/28/12	Low	0.0003	350	0.30	3	1.8	T	Einstein-Brown	49	100*	0	53	102	53	78
Bryan	06/11/11	Low	0.0003	600	0.21	17	0.6	FS	Einstein-Brown	134	99	1	1	135	2	47
Bryan	10/11/11	Moderate	0.0003	3,400	0.26	34	0.6	FS	Einstein-Brown	6,660	46	3,605	93	6,753	3,698	1,421
Bryan	12/21/11	Low	0.0003	750	0.21	17	0.6	FS	Einstein-Brown	690	41	408	3	694	411	107
Bryan	01/27/12	High	0.0003	21,200	0.21	121	0.3	FS	Einstein-Brown	141,239	99*	1,201	412	141,651	1,613	19,229
Bryan	03/24/12	High	0.0003	30,000	0.21	142	0.2	FS	Einstein-Brown	84,307	100	0	834	85,141	834	33,788
Bryan	04/13/12	Moderate	0.0003	5,000	0.7	18	1.5	T	Einstein-Brown	3,347	100	0	19	3,367	19	1,780
Hempstead	06/12/11	Low	0.0002	700	0.21	29	0.7	FS	Einstein-Brown	89	97	3	0	89	3	39
Hempstead	10/13/11	Low	0.0002	2,400	0.22	59	0.7	FS	Einstein-Brown	7,132	49	3,637	2	7,134	3,639	429
Hempstead	01/27/12	High	0.0002	16,000	0.13	134	0.2	FS	Einstein-Brown	298,766	97	8,963	540	299,306	9,503	10,369
Hempstead	02/17/12	Moderate	0.0002	4,500	0.21	69	0.6	FS	Einstein-Brown	6,779	100	0	71	6,850	71	1,621
Hempstead	03/24/12	High	0.0002	57,500	0.13	177	0.2	FS	Einstein-Brown	212,273	97	6,368	1,799	214,072	8,167	48,487
Hempstead	04/13/12	Moderate	0.0002	7,900	0.21	83	0.5	FS	Einstein-Brown	9,485	97	285	237	9,722	522	4,017
Richmond	11/10/10	Low	0.0002	2,500	0.37	31	1.5	T	Einstein-Brown	185	90	19	1	186	20	370
Richmond	01/09/12	Moderate	0.0002	7,300	0.22	55	0.7	FS	Einstein-Brown	60,744	90	6,378	91	60,835	6,469	3,022
Richmond	01/28/12	Moderate	0.0002	5,800	0.21	53	0.6	FS	Einstein-Brown	21,926	90	2,302	46	21,972	2,348	1,872
Richmond	01/30/12	High	0.0002	14,400	0.54	35	1.8	T	Einstein-Brown	120,793	90	12,683	424	121,217	13,107	9,411
Richmond	02/02/12	Moderate	0.0002	4,300	0.25	45	0.8	FS	Einstein-Brown	13,498	90	1,417	18	13,516	1,435	1,154
Richmond	03/26/12	High	0.0002	53,000	0.54	59	1.4	T	Einstein-Brown	169,341	90	17,781	7,666	177,007	25,446	81,260
Rosharon	01/10/12	Moderate	0.0002	10,500	0.38	40	1.3	T	Einstein-Brown	58,277	71	16,900	253	58,530	17,153	5,513
Rosharon	01/28/12	Moderate	0.0002	4,400	0.46	20	2.1	T	Einstein-Brown	10,224	71	2,965	121	10,345	3,086	1,880
Rosharon	01/30/12	High	0.0002	15,700	0.38	48	1.2	T	Einstein-Brown	176,853	100	0	678	177,531	678	11,699
Rosharon	03/26/12	High	0.0002	47,600	0.38	89	0.9	FS	Einstein-Brown	169,764	71*	49,232	4,045	173,809	53,277	65,763
Rosharon	05/17/12	Low	0.0002	2,100	0.23	24	1.0	FS	Einstein-Brown	455	57	196	31	485	226	497
Rosharon	07/12/12	Low	0.0002	1,500	0.23	22	1.0	FS	Einstein-Brown	1,138	100	0	12	1,150	12	279

Table 5.2: Summary of sediment transport calculations. [1]Transport modes based on the Rouse number, $z_* = w_s/(\kappa u_*)$, FS: full suspension ($z_* < 1$), T: transitional ($1 < z_* < 6.25$), BL: bedload dominated if motion ($z_* > 6.25$). *Wash load values used in the development of the sediment rating curves.

5.2 Effective discharge calculations

5.2.1 Development of the daily flow PDF

The developed rating curves were used in conjunction with the flow duration histograms (pdf of the daily flow discharge) to build the sediment transport histograms as a function of daily flow levels (fig. 2.2). The flow duration histograms, S_h (equation 2.2), were computed two different ways. In the first, the histogram was developed by manually selecting the discharge bin width and sorting the observed daily flow data. In the second, the histogram was generated objectively using the kernel density method of Klonsky and Vogel (2011).

For the manual method, the discharge bin widths were first set to an evenly spaced 25 bins over the range of observed data at each site following the recommendations of Hey (1997), and Biedenharn et al. (2000). However, when doing this, it was most often the case that the first bin in the sediment histogram, S_h, that resulted from multiplication of the flow frequency histogram with the sediment load contained by far the greatest percentage of sediment; this would result in the effective discharge being defined as the discharge equal to the midpoint discharge of the first bin. When this occurred, the number of bins was increased in increments up to a total of 40 or 50 bins in an attempt to produce a smoother histogram.

During this process of manually modifying the discharge bin widths, it was observed that the selection of the bin width greatly impacted the final effective discharge estimates. In an effort to avoid the subjectiveness of the bin width selection, a second, more objective, method for creating the flow duration histogram was used. The method used was the kernel density estimation method of Klonsky and Vogel (2011). The details of the kernel density method are discussed below.

The kernel density estimation (KDE) is a non-parametric way of building a pdf, $P_{kde}(x)$ from a random variable. The KDE is defined as,

$$P_{kde}(x) = \frac{1}{nh}\sum_{i=1}^{n} K\left(\frac{x - x_i}{h}\right) \tag{5.8}$$

where the x_i values are the individual daily discharge values, x is the discharge associated with $P_{kde}(x)$ in the resulting smoothed pdf, n is the number of measured data points, h is the bandwidth, and K is the kernel. The kernel must be a non-negative and symmetric function, i.e., $K(x) = K(-x)$, that integrates to one,

$$\int_{-\infty}^{\infty} K(x)\,dx = 1 \tag{5.9}$$

There are several different kernel forms that can be used, e.g. the uniform kernel where $K(x) = 0.5$ for $-1 \leq x \leq 1$ and zero elsewhere. For this analysis we have used the normal Gaussian kernel,

$$K(x) = \frac{1}{\sqrt{2\pi}} e^{-x^2/2} \tag{5.10}$$

In equation 5.8, the bandwidth h is a smoothing parameter that strongly influence the shape of resulting density function. Bandwidth values that are too small will results in a density function that is not smooth, and values that are too large will result in over smoothing. The desired

bandwidth is one that produces a smooth density function that well represents the overall distribution of the data. The most common method used for selecting this parameter is to find the bandwidth value that minimizes the mean integrated squared error, E:

$$E = \int_{-\infty}^{\infty} [P_{kde}(x) - P(x)]^2 dx \tag{5.11}$$

where, $P(x)$ is the true distribution of the data. If a Gaussian basis function is used to approximate the measured data, and if the underlying density being estimated is Gaussian, then it can be shown that the optimal choice for h is:

$$h = \left(\frac{4\sigma^5}{3n}\right) \simeq 1.06\sigma n^{\frac{-1}{5}} \tag{5.12}$$

where σ is the standard deviation of the data (Silverman, 1998).

In this analysis, MATLAB was used to develop the P_{kde} of the daily discharge data. In MATLAB, P_{kde} was evaluated at 100 equally spaced points that covered the range of the observed flow rates using the command `ksdensity(x)`. For example, `[f,x_i] = ksdensity(x)`, where `f` was the vector of density values evaluated at the points `x_i`. The calculations were done using a normal kernel function (equation 5.10) and a bandwidth window parameter (width) that is a function of the number of points in `x` (equation 5.12). Figure 5.2 shows the resulting daily flow pdfs for Waco and Richmond using both the manual and kernel density estimate.

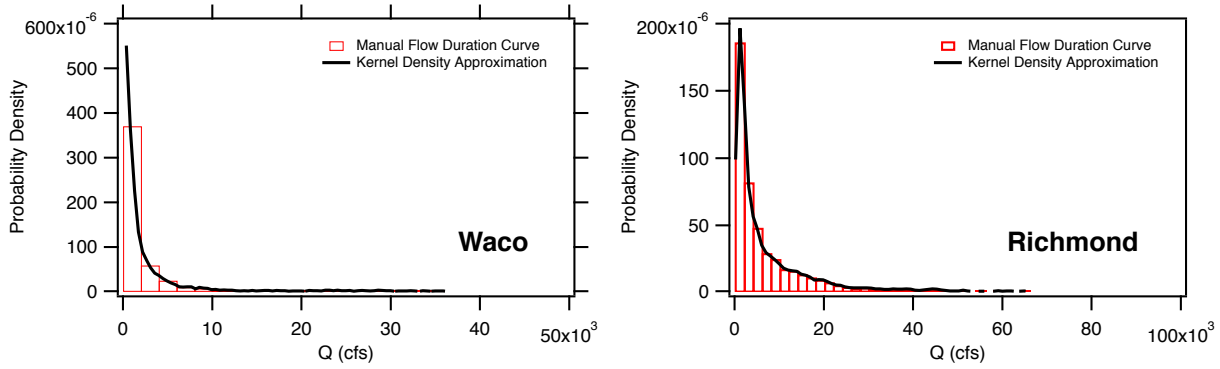

Figure 5.2: Example of the manual and kernel density estimate derived daily flow pdf for the period of analysis.

Overall the kernel density estimate derived distributions f_Q, tended to be inline with the manually developed pdfs once the bin width of the manually developed pdfs had been modified. The biggest differences between the two methods are that, (1) the kernel density estimate method requires no modification of the bin number/width, and (2) that the kernel density estimate should be less sensitive to single large discharge events since it produces a smoothed pdf. One practical difference between using the KDE and manually developed histograms or pdfs is that it is easier to manually develop a histogram of the daily discharges (frequency of occurrence of a discharge within the bin range), whereas the KDE produces a probability density function. The difference between a pdf and a histogram is that the P_{kde} integrates to 1 whereas a histogram does not. Both a manually developed histogram and pdf will yield the same effective

discharge measure in the sediment load histograms since the overall shape of the pdf and histogram of equal bin sizing are the same. However, the values of the load histogram developed with a histogram will be different than those developed using a pdf.

5.2.2 Sediment transport effectiveness distributions

Effective discharge estimates, Q_e, were made directly from sediment transport effectiveness histograms, S_h (Wolman and Miller, 1960), that were developed using both the manual and kernel density pdfs of the flow. The S_h distributions were developed by multiplying the load at a particular discharge as estimated by the rating curves with the pdf of the daily flow discharge (equation 2.2). This was done independently for the bed load, Q_b, and suspended bed material load, Q_{sbm} as follows:

$$S_{h:sbm} = Q_{sbm} f_Q \tag{5.13}$$

$$S_{h:b} = Q_b f_Q \tag{5.14}$$

with the total transport effectiveness distribution being the summation of the bed and suspended load,

$$S_h = S_{h:sbm} + S_{h:b} \tag{5.15}$$

For the manually developed histograms, the discharge at the midpoint of the discharge bin was used to calculate that daily loads from the rating equations. For the kernel density method, the Q values used corresponded 100 regularly spaced values for which f_Q was calculated. The effective discharge was determined from the sediment load histogram as the discharge associated with the peak or highest value of S_h. The sediment effectiveness distribution were calculated using the rating curves developed using (1) only data from this study, (2) using all available USGS data plus the data from this study, and (3) using the SAMwin rating curves. Coefficients for all of these rating curves can be found in Table 5.1. Figures 5.3 and 5.4 show these effectiveness distributions developed using the data obtained in this study, and the values of effective discharge obtained using all three of the different rating curve sets are given in Table 5.3.

Very little difference was found in the computed effective discharge when using the rating curves developed with only the UH measured data for the suspended bed material compared to those developed using the UH plus USGS data (Table 5.3); the one exception to this is at Richmond. Therefore, in moving forward with the analysis, only the rating curves developed with the measured data from this study will be used.

In addition to the effective discharge, we also calculated the half-load sediment discharge, $Q_{1/2}$ from cumulative distributions of the sediment moved as a function of discharge. These values along with the cumulative curves for the amount of water and sediment moved during the analysis time period at each stations as a function of flow discharge are shown in figures 5.5 and 5.6. The plots shown in these figures are similar to the suggested summary plots of Klonsky and Vogel (2011) (i.e., figure 10 in their paper). The plots can be used to easily see what the fraction of water moved by flows less than (or greater than) a particular discharge is and what percentage of sediment moved this corresponds to. For example, at Highbank (figure 5.5), the figure can be used to see that about 50% of the water volume is moved by discharges less than 10,000 cfs, but that discharges less than 10,000 cfs only transport about 30% of the sediment passing the station. The plots can also be used to show what the total fraction of sediment

moved by flows equal to and less than the effective discharge. For example, at Highbank, flows equal to and less than the effective discharge are responsible for transporting about 80% of the total sediment load.

Station	Q_e using Manual $f_e(Q)$		Q_e using Kernel $f_e(Q)$		Different Q_e values by method?		
	Measured [cfs]	SAM [cfs]	Measured [cfs]	SAM [cfs]	Manual vs Kernel $f_e(Q)$	Measured vs SAM	UH vs USGS+UH[3]
Waco	28500	28500	29000	29000	no	no	-
Highbank	30500 (33000)[1]	30500	33000 (33000)	33000	no	no	no[4]
Bryan	17000	17000	9000	44000	yes	no[2]	-
Hempstead	18000	18000	18000	18000	no	no	-
Richmond	45000 (65000)	45000	44000 (65000)	44000	no	no	yes
Rosharon	46000 (46000)	46000	63000 (63000)	63000	yes	no	no

Table 5.3: Comparison of calculated effective discharge using both the manual and kernel density estimation for $f_e(Q)$ along with the effective discharge values obtained using the total load rating curves via SAM. The right three columns give an indication of how dependent the calculated Q_e value is on, (1) the method used to develop $f_e(Q)$, (2) whether or not measured suspended load plus calculated load is used instead of a single calculated total load, and (3) whether or not all of the historic USGS data is used in addition to the data measured in this study for suspended bed material.
[1]Values in parenthesis represent the effective discharge obtained using all of the available USGS data in developing the rating curves at Highbank, Richmond, and Rosharon.
[2]For the kernel derive $f_e(Q)$ this should be "yes."
[3]Results were the same for both the manual and kernel derive $f_e(Q)$.
[4]For the manually derived $f_e(Q)$ this should be "yes."

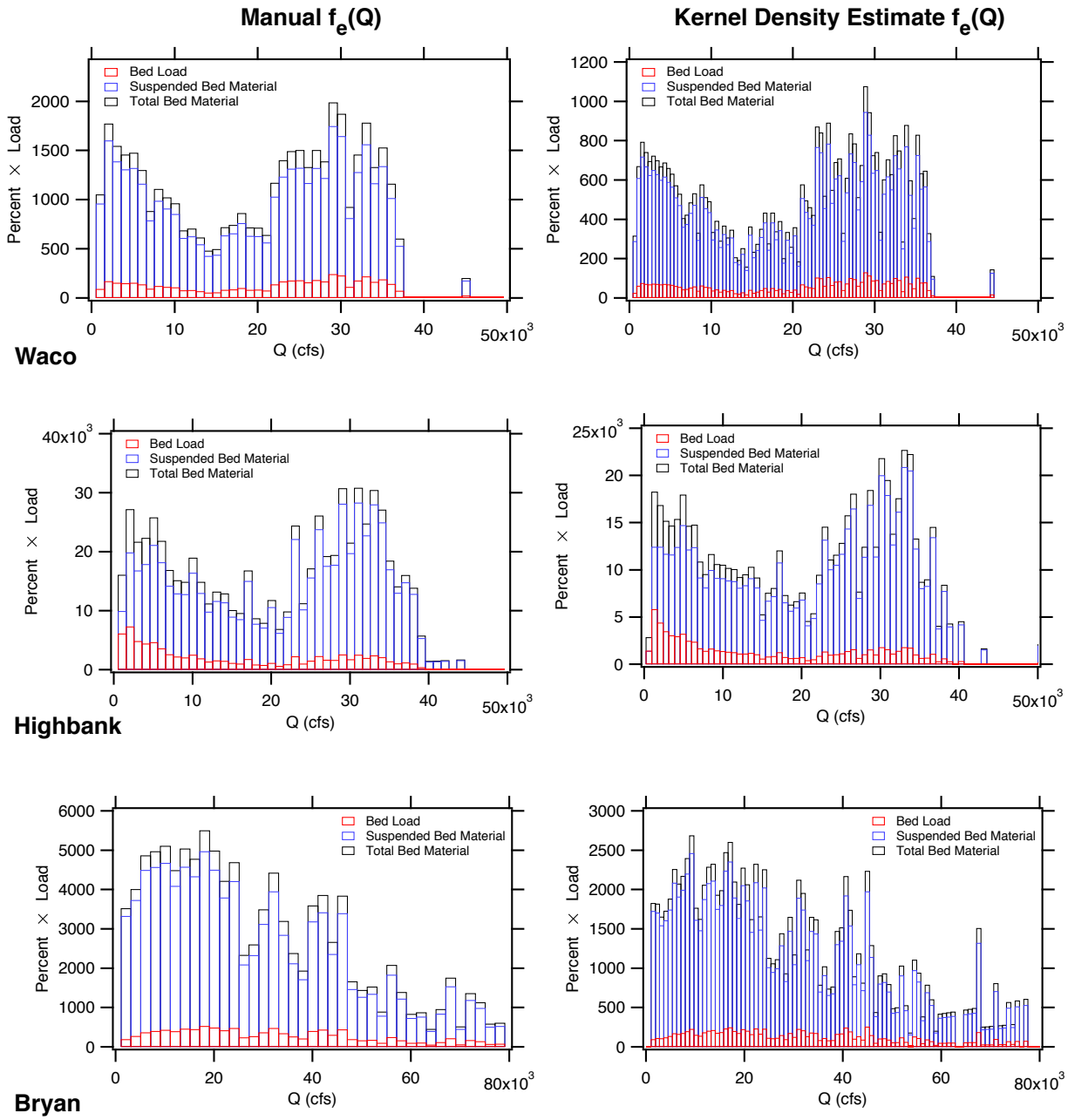

Figure 5.3: Sediment transport effectiveness distributions for Waco, Highbank, and Bryan using both the manual and kernel density estimate derived daily flow pdfs.

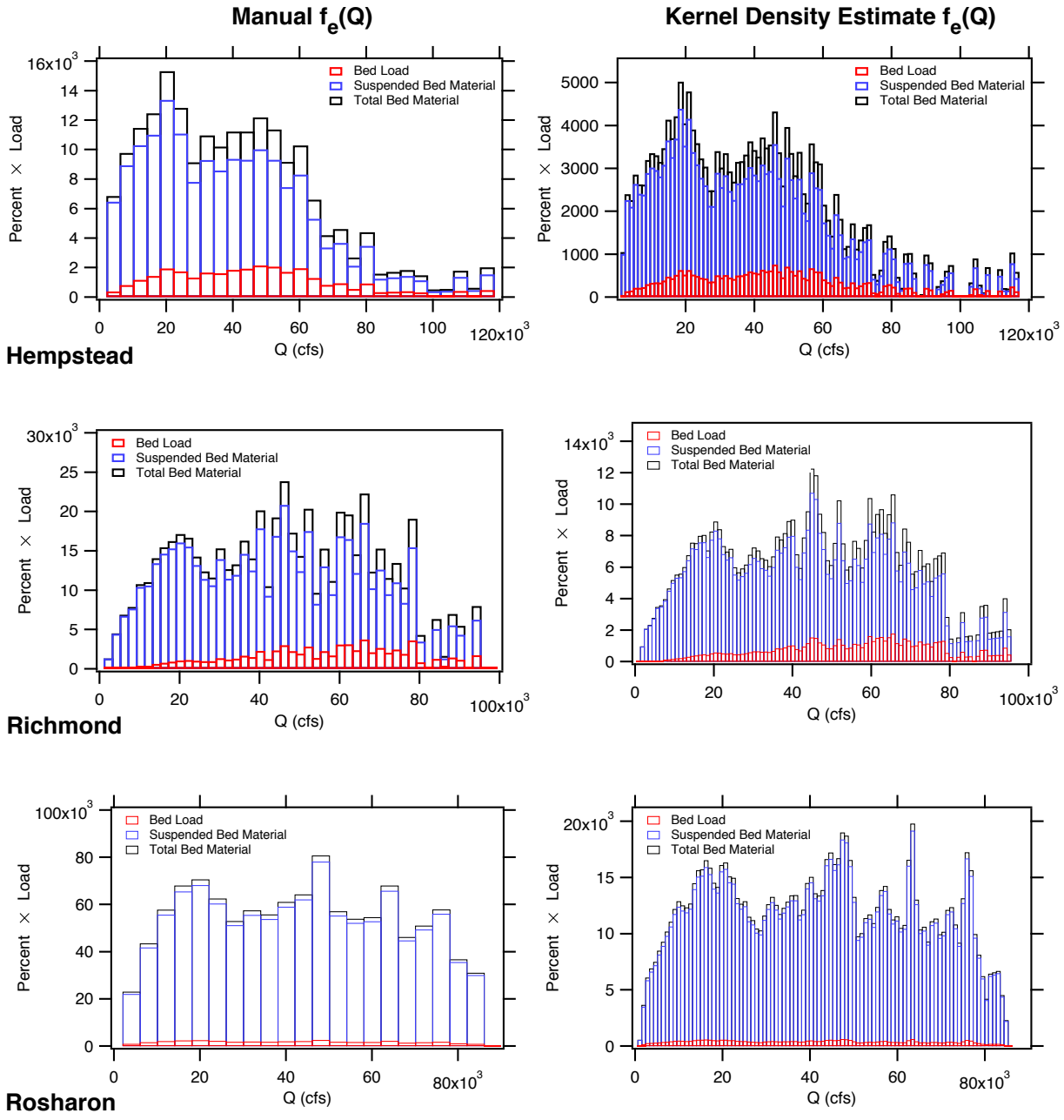

Figure 5.4: Sediment transport effectiveness distributions for Hempstead, Richmond, and Rosharon using both the manual and kernel density estimate derived daily flow pdfs.

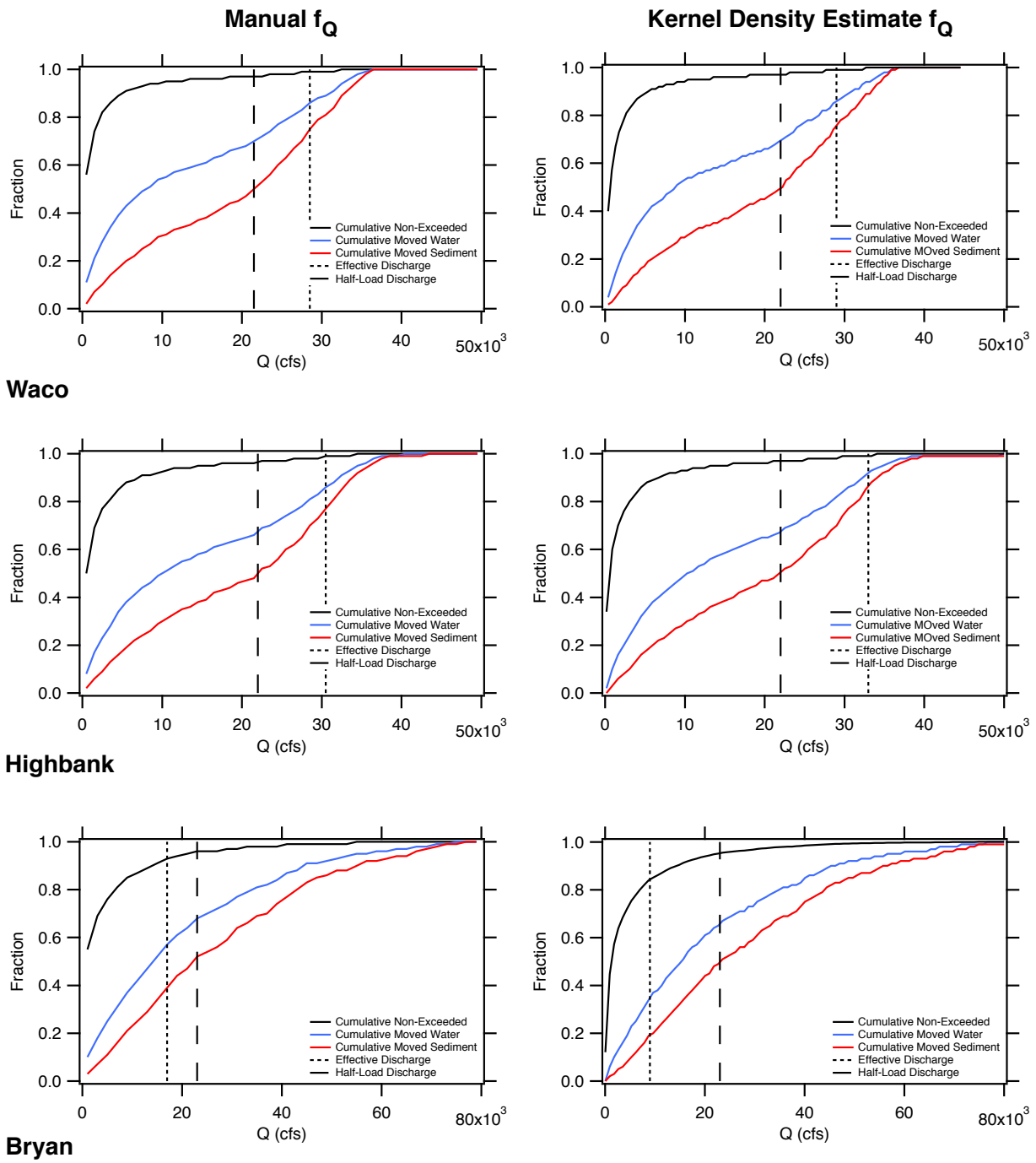

Figure 5.5: Summary plots showing the cumulative fraction of flow and sediment moved as a function of discharge, the flow non-exceedance curve, the sediment effective and half-load discharges for Waco, Highbank, and Bryan using the manual and kernel density estimate derived daily flow pdfs.

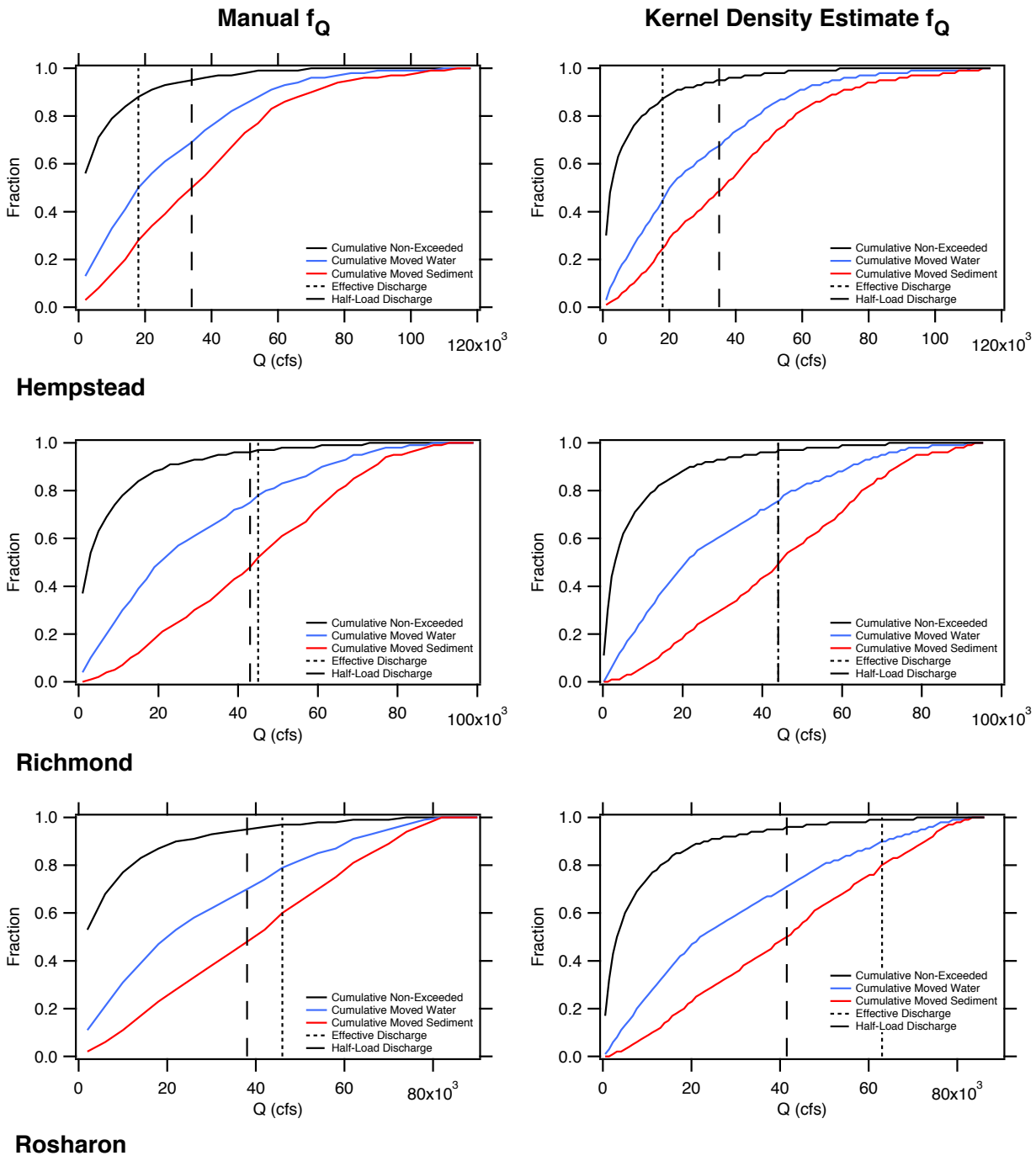

Figure 5.6: Summary plots showing the cumulative fraction of flow and sediment moved as a function of discharge, the flow non-exceedance curve, the sediment effective and half-load discharges for Hempstead, Richmond, and Rosharon using the manual and kernel density estimate derived daily flow pdfs.

5.2.3 Discussion on the effective discharge estimates

A summary of the effective discharge and half-load discharge data along with the fraction of time that flows exceeded the effective discharge, the fraction of sediment carried by flows less than the effective discharge, and the calculated return period of the effective discharge for both the manual and kernel density estimation methods are given in table 5.4. Effective discharge calculated using the two different methods for developing f_Q were fairly equivalent; though at Bryan, the manually developed f_Q produced a greater estimate of Q_e. Because of the seemingly unreasonable small Q_e estimate at Bryan with the kernel method, we suggest that the load histograms obtained with the manual density estimate of the daily flow pdf are the best for estimating the effective discharge and half-load discharge on the lower Brazos.

	Manual $f_e(Q)$					Kernel Density Estimate of $f_e(Q)$				
Station	Q_e [cfs]	$Q_{1/2}$ [cfs]	PT Q_e exceeded	PS carried by $Q < Q_e$	T_R [yr]	Q_e [cfs]	$Q_{1/2}$ [cfs]	PT Q_e exceeded	PS carried by $Q < Q_e$	T_R [yr]
Waco	28500	21500	1	75	2.9	29000	22000	1	74	2.9
Highbank	30500	22000	1	77	2.3	33000	22000	1	85	2.6
Bryan	17000	23000	7	39	1.2	9000	23000	16	19	1
Hempstead	18000	34000	12	28	1.1	18000	35000	13	24	1.1
Richmond	45000	43000	3	52	1.4	44000	44000	3	50	1.4
Rosharon	46000	38000	3	60	1.5	63000	41500	1	80	2.3

Table 5.4: Effective discharge summary table. PT: percentage of time that the effective discharge, Q_e is exceeded. PS: percentage of sediment carried by flows less than the effective discharge. T_R: return period of the effective discharge.

The calculated effective discharges range between the expected 1 and 2 year return period for the lower four stations, but Q_e for Waco and Highbank were associated with relatively larger flow events with return periods between 2 and 3 year (table 5.4). At these two sites, the effective discharge is exceeded only about 1 percent of the time. This would seem to indicate that the largest releases from the upstream dams are setting the morphologic state and effective discharge at the Waco and Highbank sites. Moving downstream to the four lower gages, this trend in effective discharge does not remain. In fact, based on the analysis methods used, there does not seem to be a clear consistent trend in the effective discharge estimates. Q_e does not systematically stay the same, increase, or decrease with drainage area. Instead, the Q_e calculation seems to be strongly dependent on the local sediment conditions and observed flow history. Figure 5.7 shows the state of the river at Hempstead during a flow event roughly equivalent to the calculated effective discharge.

Very few of the developed sediment load histograms, S_h, were nice smooth continuous distributions as conceptualized in figure 2.2 and in Wolman and Miller (1960); in fact, most were quite uneven with multiple peaks. In selecting the effective discharge values stated in tables 5.3 and 5.4 from the load histogram, the maximum value of S_h was simply selected without regard to any smoothed trending pattern. Biedenharn et al. (2000) suggests that when the data does not produce a smooth continuous histogram, that a smoothed line can be drawn in by eye through the bins and the effective discharge can then be taken as the peak in the smoothed

Figure 5.7: The Brazos River at the Hempstead station on January 27, 2012. The picture was taken in the afternoon at a flow rate of Q = 16,000 cfs, which was approximately equal to the effective discharge (table 5.4. The measurements made at this time were done during the rising limb of the event hydrograph. Measured concentrations on this day were the highest of any observed at Hempstead (wash load was 97%).

curve. Following this suggestion, smooth curves were drawn through the histograms (figure. 5.8). Drawing these curves was quite subjective. For example, multiple curves could be envisioned as "fitting" the data for each histogram depending on the interpretation of the one drawing the histogram. Because of the subjectiveness in drawing these curves, we have decided not use the smoothed histograms in determining the effective discharge. However, the discharges and return periods associated with the various peaks in the drawn-in histograms are given in Table 5.5.

Part of the difficulty associated with drawing in the smooth curves is that it most the sediment load histograms have, what appears to be, two peaks. One of the peaks is usually higher than the other, but there seems to be two systematic peaks in each of the load histograms. These two peaks may be indicating that the overall load histograms is a superposition of a two distinct load distributions. One of which is associated with lower flows ($Q < 1_{1.5}$), and one associated with higher flows ($Q > Q_{1.5}$). This superposition idea is supported by the fact that there is typi-

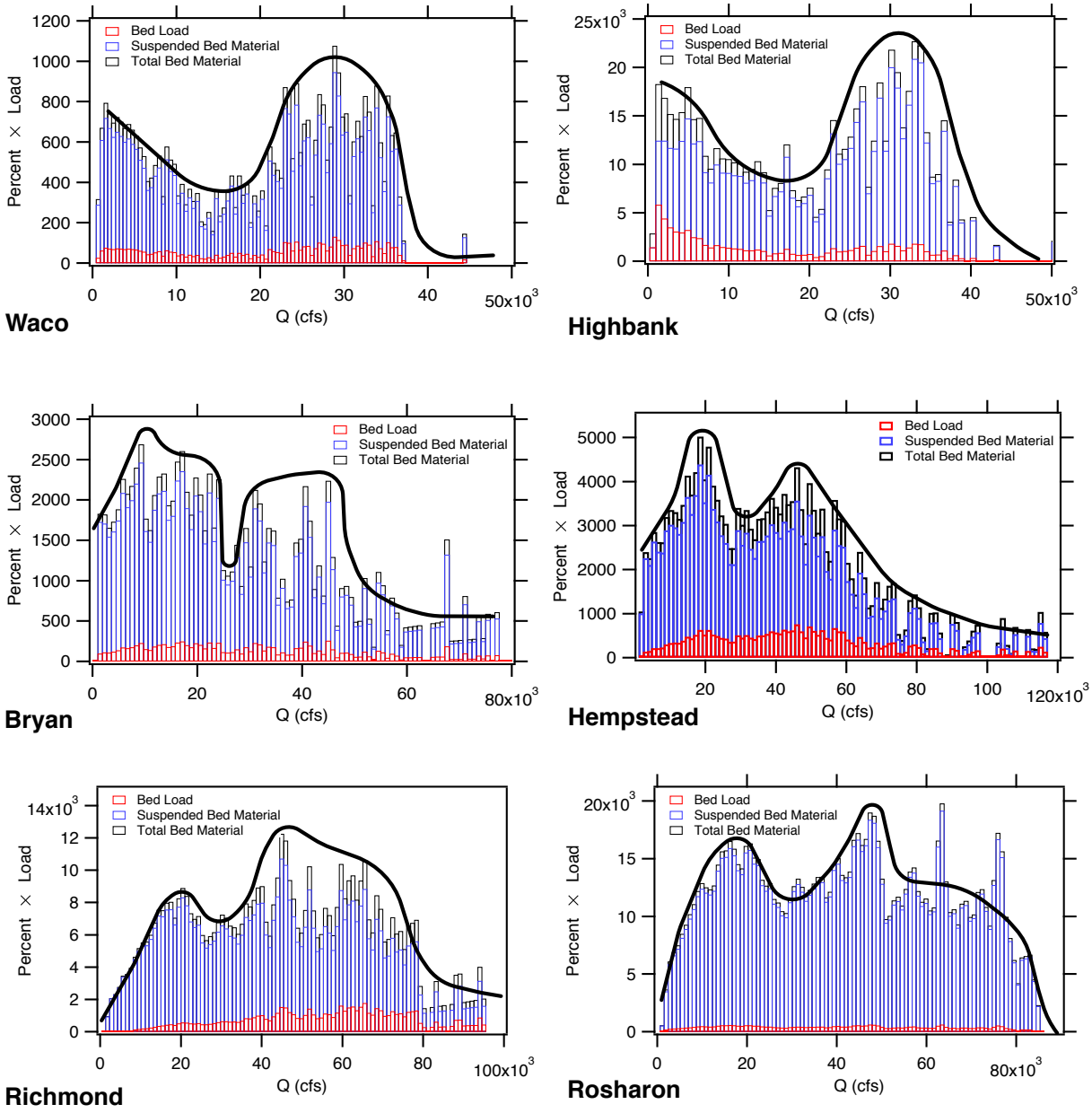

Figure 5.8: Sediment histograms developed using the kernel flow pdf superimposed with possible drawn in continuous transport effectiveness curves.

cally a local minimum in S_h around discharge values that fall just above the slope break in the cumulative water transported curves in figures 5.5 and 5.6 around the 50% to 60% of total water transported mark. These values work out to be approximately 13,000 cfs at Waco, 20,000 cfs at Highbank, 24,000 cfs at Bryan, 27,000 cfs at Hempstead, at 27,000 Richmond, and 28,000 cfs at Rosharon; these discharges fall into the 1 to 1.5 return period range at each of the sites. Interestingly enough, these minimums in the S_h distributions are approximately equal the half-load discharges $Q_{1/2}$ at Highbank, Bryan, and Hempstead (table 5.4). This would indicate that approximately half of the bed material is moved by larger infrequent flows and half by the lower

$f_e(Q)$ peaks in smoothed histogram				
	First		Second	
Station	Q [cfs]	T_R [yrs]	Q [cfs]	T_R [yrs]
Waco	1300	<1	29000	2.9
Highbank	4500	<1	33000	2.6
Bryan	9000	1	44000	1.8
Hempstead	18000	1.1	45000	1.5
Richmond	19000	1.1	44000	1.4
Rosharon	19000	1.5	47000	2.3

Table 5.5: Effective discharge estimates by peak order using a smoothed histogram along with either associated return periods.

more frequently observed flows, with a comparatively small amount of sediment being moved by the 1.5 year return period flow.

Again, the higher flows are more influential at the upstream Waco and Highbank stations, while the lower flows are more influential at the downstream gages. At Rosharon, the general shape of the load histogram seems to indicate that the lower flows are more influential. However, the largest peak in the histogram is associated with the higher flows, even though the peak is rather narrow (figure 5.8).

5.2.4 Relation between effective discharge, half-load discharge, and bankfull discharge

A reasonable question to ask is how the calculated effective discharges computed with the total load sediment histogram (equation 5.15) compare with (1) the effective discharge calculated using only the suspended bed material load histogram (equation 5.13), (2) the sediment half-load discharge calculated using total load, (3) the bankfull discharge, and (4) the 1.5 year return period flows at each of the sites. Calculation of the half-load discharges was done using the cumulative sediment loading curve as a function of discharge as described above.

A description of how each of these values was calculated has been given above for all discharges other than the bankfull discharge. The bankfull discharge, Q_{bf} is defined as the discharge that just fills the main channel up to the top of its banks with water. There are two primary methods for calculating the bankfull state. In the first, the bankfull cross section can be defined in the field using the geometric properties of the cross section and vegetation indicators. The discharge can then be calculated knowing the bankfull geometry, the channel slope, and the roughness coefficient (such as the Manning n value). It can also be defined using a measured range of discharges and geometric properties, e.g., stage or top width as a function of discharge. In this study, we have calculated the bankfull discharge using USGS measurements of discharge and cross sectional top width, T. With this second method, the bankfull state is defined as the discharge after which there is a slope break in the $T = T(Q)$ functionality (or break in the functionality of stage with discharge). The slope break can be viewed as the discharge at which water begins to spill out of the main channel and onto the wider flood plane. This break will therefore manifest itself as a increase in the rate of top width expansion with discharge.

Plots of $T = T(Q)$ are shown using the available data at each of the six stations in figure 5.9.

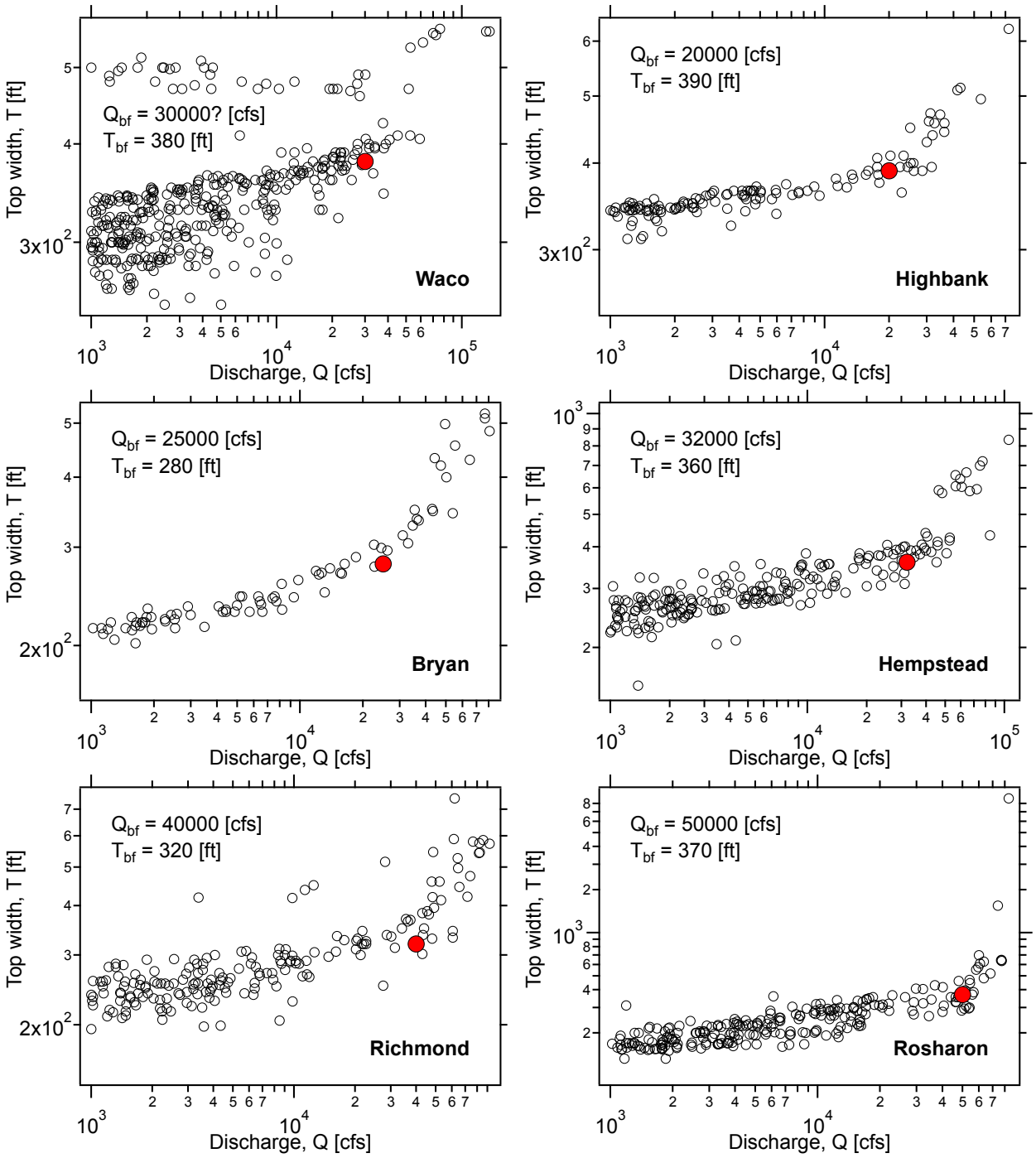

Figure 5.9: USGS measured top width and discharge at each of the six stations. The red markers indicate the visually identified bankfull state.

The bankfull state at each site was selected from the plots in figure 5.9 as the theoretical intersection of two straight lines fit to each of the two different sections of $T = T(Q)$ functionality. The bankfull slope break was most clearly defined at Highbank, Bryan, and Hempstead.

While less defined, Richmond and Rosharon also exhibited a transition in the slope. The lack of definition in the bankfull condition at Richmond and Rosharon is likely due to the incised nature of the channels at these locations and the lack of physical measurements at flows high enough to cause the Brazos to crest the top of the main channel banks. No clear trend or change in trend was found in the Waco data. The bankfull states calculated from these plots are listed in Table 5.6 along with the other dominant discharge estimators. Excluding Waco, the bankfull discharge increases continuously with an increase in drainage area. In general, the bankfull state is close to the 1.5 year return period flow, especially when $Q_{1.5}$ is calculated using all of the available data.

	Total Load[1]		Suspended[2]	Pure Flow Metrics		
Station	Q_e [cfs]	$Q_{1/2}$ [cfs]	Q_e [cfs]	Q_{bf} [cfs]	$Q_{1.5}$ (20 yrs) [cfs]	$Q_{1.5}$ (All yrs) [cfs]
Waco	28,500	21,500	28,500	30,000[3]	16,300	24,800
Highbank	30,500	22,000	30,500	20,000	20,000	21,200
Bryan	17,000	23,000	17,000	25,000	28,800	28,800
Hempstead	18,000	34,000	18,000	32,000	45,900	40,700
Richmond	45,000	43,000	45,000	40,000	51,400	44,500
Rosharon	46,000	38,000	46,000	50,000	46,300	44,000

Table 5.6: Final effective discharge, Q_e, half-load discharges, $Q_{1/2}$, and bankfull discharges, Q_{bf}, at each of the six stations.
[1]Effective and half-load discharges calculated using the total load histogram, $S_h = S_{h:sbm} + S_{h:b}$.
[2]Effective discharges calculated using the suspended bed material load histogram only, $S_{h:sbm}$.
[3]An estimate. No clear break in the relationship between top width and discharge at Waco (figure 5.9).

As a first comparison, one can note that the effective discharge calculated using the total load histogram aligned with those from the suspended sediment at all six sites, and that the calculated effective discharge is more variable progressing downstream than any of the other measures. Past this, generalizations about the relative magnitude of the various discharge measures can be made, but these generalizations do not hold true in every case. For example, $Q_{1/2}$ is approximately equal to the Q_{bf} with the exception of the Rosharon site were $Q_{1/2}$ is smaller than Q_{bf}. The effective discharge, on the other hand, is approximately equal to the bankfull discharge at Waco, Richmond, and Rosharon, but is significantly different for the middle stations of Highbank, Bryan, and Hempstead. In general, the 1.5 year return period discharges are equal to slightly greater than the bankfull discharge and half-load discharge. Water surface elevations corresponding to each of the four measures of dominant discharge are plotted for each cross section in figures 5.10 and 5.11.

In this analysis, the effective discharge estimates showed no consistent downstream trend or consistent trend in relation to the other possible measures of dominant discharge. This might be due to either a true bimodal distribution in the sediment load histograms, or it may somehow be an outcome of the methodology used in calculating the effective discharges. In contrast, the geometric properties of the Brazos from Waco to Rosharon do not change all that much. The width of the river away from the road crossing increases slightly with drainage area up to Richmond and then decreases at Rosharon. However, the changes in width are not extreme if the

Rosharon site is excluded (figure 4.7). The slope decreases slightly moving downstream but no major shifts in bed material grain size were observed. The largest change in the geometry of the river cross sections was in the depth. Moving downstream the geometric depth of the channel (top of bank to average bottom of channel) increases, with a doubling of the Waco depth by the Rosharon crossing. An increase in the depth would be expected since the width does not change significantly, but the flows increase substantially with an approximate doubling of $Q_{1.5}$ from Waco to Rosharon (Table 5.6).

Because the cross sectional properties and slope of the Brazos change rather slowly and systematically downstream, it is possible that the current channel cross-sectional properties are not reflective of the effective discharge using the methodology and data from this study. For the sites considered, it seems as though the half-load discharge may be more reflective of the channel setting flows.

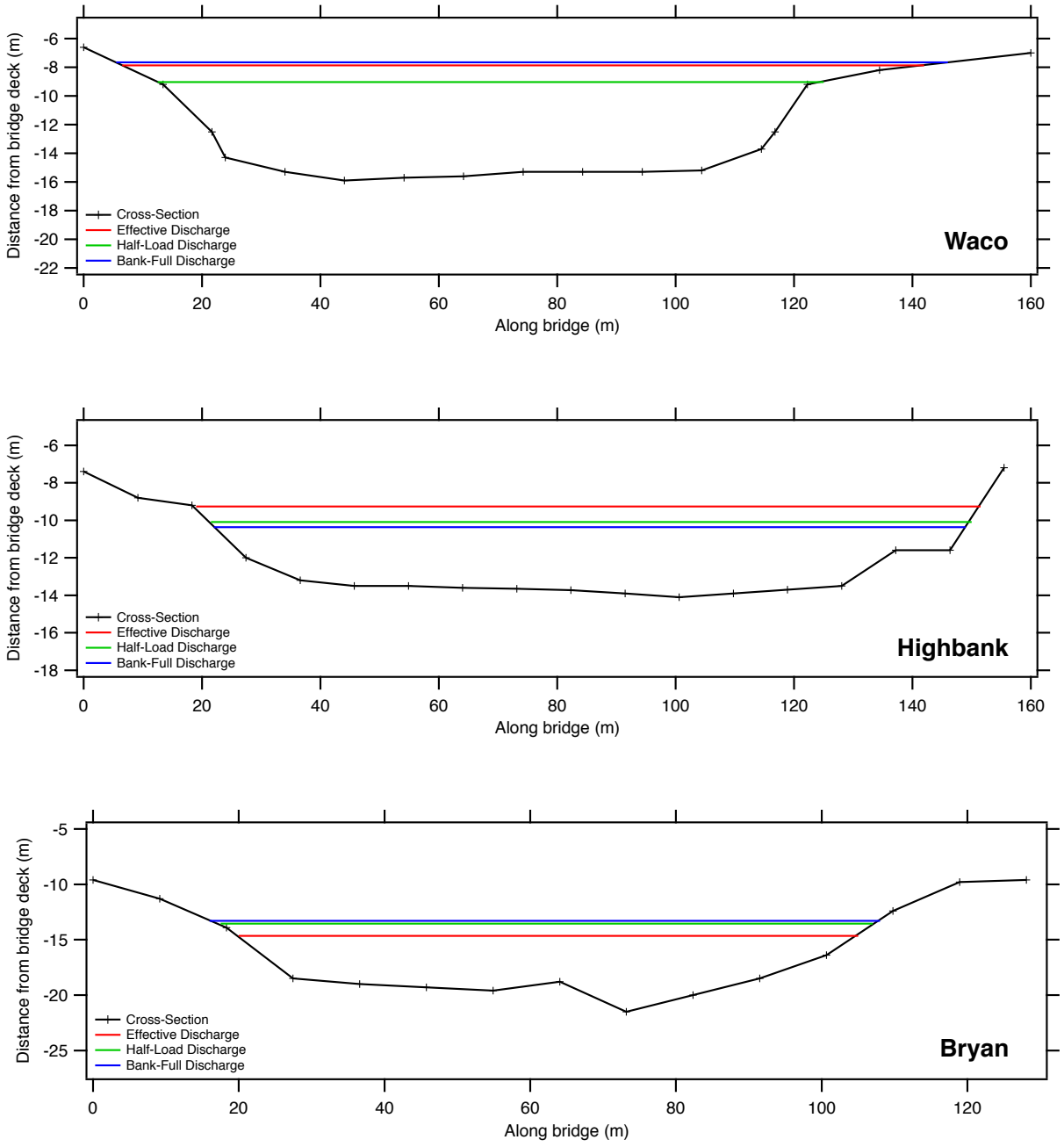

Figure 5.10: Cross section plots at Waco, Highbank, and Bryan with the water surface elevations for the effective, half-load, bankfull, and 1.5 year return period flows.

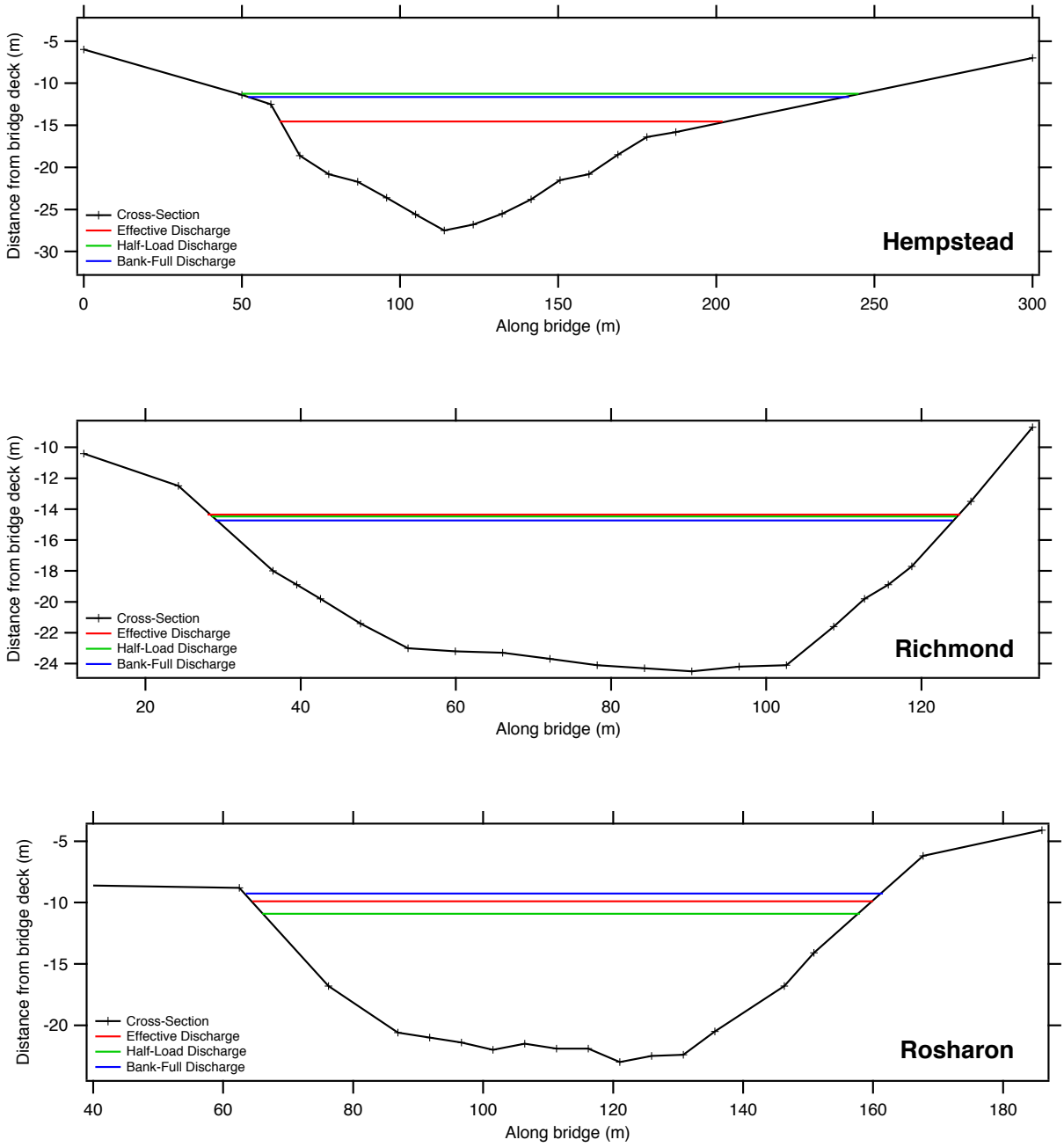

Figure 5.11: Cross section plots at Hempstead, Richmond, and Rosharon with the water surface elevations for the effective, half-load, bankfull, and 1.5 year return period flows.

5.3 Annual sediment yield

The annual sediment yield at each station was calculated using the daily flow data and the rating curves developed for bed load, suspended load, and total suspended material (suspended load + wash load). These were integrated over a one-year time period to produce a load associated with each year. Plots of the yearly loads from January 1, 1990 to December 31, 2009 are shown below in figure 5.12. In general, the total yearly bed material load increases moving downstream. The exception to this is the Highbank station. The likely cause of this is the poor correlation in the suspended bed material load rating curve that results in unreasonably high yields at low flows.

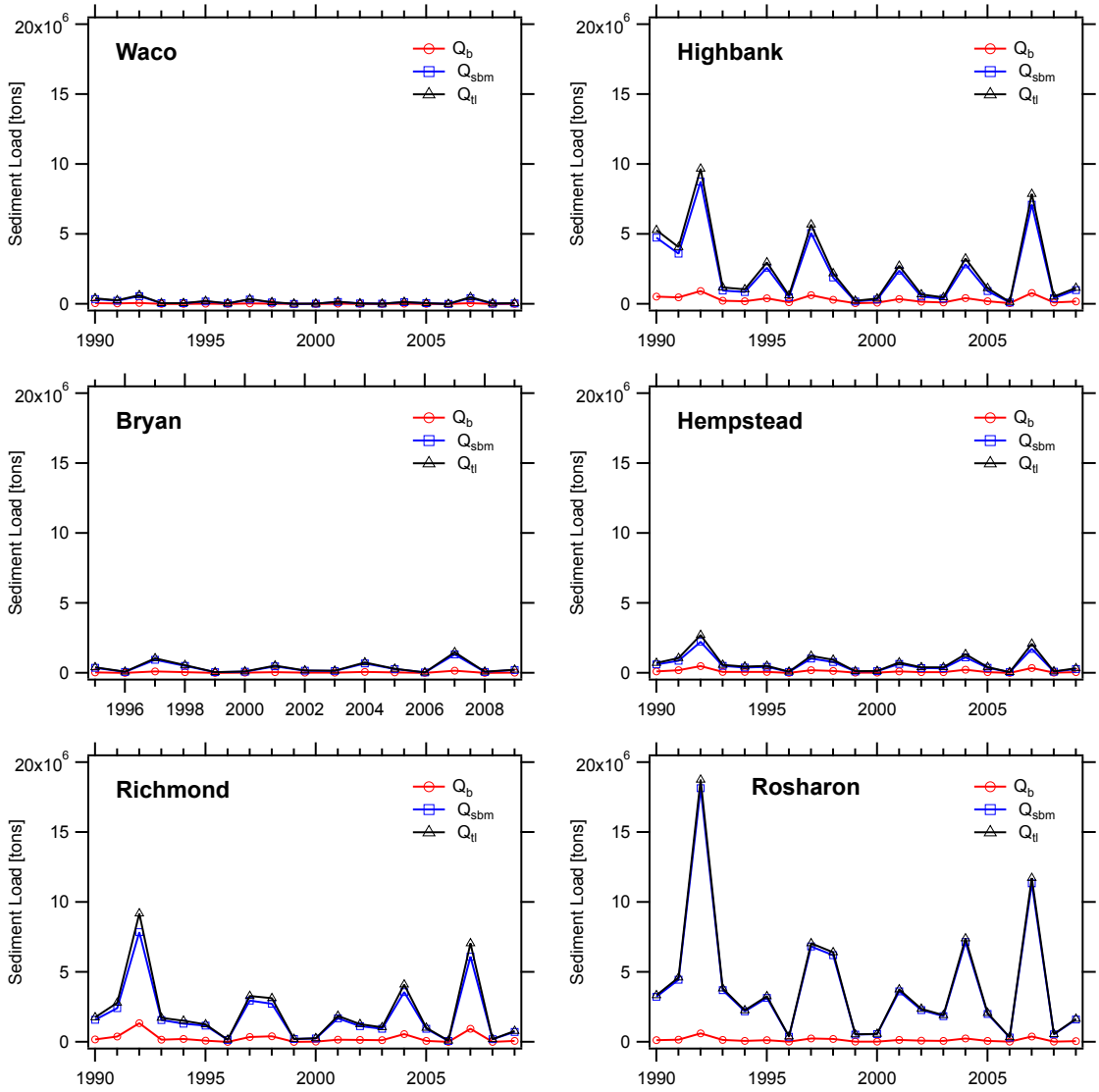

Figure 5.12: Yearly bed material loads at each of the six stations from 1990 through 2009. Q_b is the calculated bed load, Q_{sbm} is the suspended bed material load, Q_{tl} is the total bed material load, $Q_{tl} = Q_b + Q_{sbm}$.

6 Conclusions

6.1 Summary

The effective discharge was calculated at six stations along the Brazos River using historic USGS daily flow data along with rating curves developed from measured and historic USGS suspended sediment data and calculated bed load transport rates. Measurements for the analysis of channel cross sectional properties, bed sediment, and suspended sediment concentration were made primarily between October 2011 and July 2012 following a year of drought throughout Texas. The effective discharge estimates were made using probability density functions of the daily discharge created using histograms with manually set bin width and the kernel density estimation method (Klonsky and Vogel, 2011). The advantage of the kernel density estimate in defining the flow pdf is that it is objective and that it can produce a smoothed function. Sediment half-load discharges and cross sectional bankfull discharges were also calculated.

6.2 Main findings

A summary of the calculated effective discharge values can be found in table 5.6 along with other measures of dominate discharge such as the half-load discharge, the bankfull discharge, and the 1.5 year return period discharge for each station. Results showed that the calculated effective discharges varied significantly from station to station; ranging from 17,000 cfs at Bryan to 45,000 cfs at Richmond to 46,000 cfs at Rosharon. Examining the sediment load histograms seems to indicate that large changes in effective discharge from station to station could be reflective of a bimodal sediment load histogram where a significant portion of the sediment moves under two distinct flow classes. One of the classes being composed of relatively low flows (less than 20,000 cfs at most stations) and the other of relatively high flows (greater than the 1.5 year return period flow), but with little sediment being moved at flows between these two classes. At one station the high flow class may dominate while at the next station, the low flow may have a larger fraction of sediment moved, resulting in the large change in effective discharge estimate from station to station.

While the calculated effective discharge does varied from station to station, the current cross sectional properties of the Brazos over the reach examined has a more systematic trend and remains relatively unchanged in a downstream progression. The channel width and bed material grain size distribution both changed very little from station to station; the Rosharon reach is an exception to this with the width decreasing substantially. The channel geometric depth (top of bank to average of channel bottom) at the crossing and the flood flow statistics for the 1.5, 5, and 10 year flood flows both roughly doubled from Waco to Rosharon. Over this distance, drainage area increased and slope decreases (though the slopes used in the analysis where calculated from DEMs and not local measurements).

Other items of note with respect to the effective discharge calculation were that the calculated discharges were, (1) fairly insensitive to whether or not the newly measured suspended sediment data was supplemented with the historic USGS data when developing the rating curves

for the suspended sediment; (2) generally independent of the method used to develop the pdf of the daily flow (exceptions to this were Bryan and Rosharon); and (3) generally insensitive to whether or not measured data was used in developing the rating curves for suspended sediment load (only 1 out of 6 stations produced different Q_e values when using only the Engelund and Hansen (1967) total load equation in SAMwin). The lack of Q_e dependence on use of current versus historic suspended sediment data in development of the rating curve is likely a result of two factors. The first being that the measured suspended load data associated with this project fell within historically observed sediment load values recorded by the USGS. The second contributing factor might be that the form of the flow frequency histogram (or pdf) may play a stronger role than the exact form of the suspended load rating curves in determining the effective discharge; the ability to predict that effective discharge with the Engelund and Hansen (1967) formulation in SAMwin in all but one site supports this second reason.

If a single discharge were to be picked as the dominant discharge for the entire lower Brazos (i.e., that discharge for which the river is morphologically responding to) Q = 30,000 cfs might be a good choice. The average half-load discharge for all six station is approximately 30,000 cfs, and this value roughly corresponds with the bankfull discharge for the four upstream stations. The bankfull state and $Q_{1.5}$ at Richmond and Rosharon were 10,000 to 20,000 cfs higher than 30,000 cfs mark. However, it is possible that Brazos is incised at these two stations to accommodate the large flood waters, but that the lower flows are still more responsible for maintaining the channel.

In addition to the effective discharge estimate, the developed rating curves were used to calculate the daily total bed material load over the 20 year period of investigation. The loads were then integrated over each calendar year to produce a total yearly sediment yield at each station. In general, yearly loads increase with progression downstream and vary significantly from year to year.

Sediment histograms and yearly yields using the total transported sediment (bed material plus wash load) were also calculated for each station. This data is presented in Appendix A. Of note from the sediment histograms produced with the kernel density estimation method is that the discharge associated with the peak in the histogram varies more smoothly in a downstream progression than it does when only the bed material is used in development of the histogram (figs. A.1, A.2 and table A.1). The discharge associated with this peak progresses from 29,000 cfs at Waco to 63,000 cfs at Rosharon.

6.3 Further work

An item for further investigation, is to explore the question of whether or not the effective discharge, as historically calculated, is a good measure of the dominant channel forming discharge in muddy coastal systems such as the Brazos River from Waco to the Gulf of Mexico. The vast amount of sediment traveling in the Brazos is silt and clay material which is all neglected in the effective discharge calculations. The reasoning for removing the silt and clay material in the analysis is the assumption that material of this size will stay in suspension at all points in time and not significantly interact with the bed or banks. However, it is not readily clear without further analysis if this is the case for highly muddy low-slope systems like the Brazos. If a strict definition of wash load is taken as that material in suspension that does not interact with the bed, then the demarcation for wash load should vary as a function of turbulence levels. Hence,

what is wash load at high flows might not be wash load at lower flows. No altering of the wash load cut off to reflect the flow state has been done in the presented analysis.

Possibly related to this was the trend towards fining of the measured suspended grain size distribution with increasing discharge at some of the measurement stations. One reason for an overall shift in the mean of the suspended load could simply be due to greater loading of fine sediment coming in from runoff over the fields. An overall larger fraction of fine material relative to the sand load would cause a fining of the suspended sediment grain size statistics. This may help to explain some of the measured data. However, for other samples, the presence of sand, and not just the fraction of the total concentration, also decreased with discharge. This is harder to explain. An unpublished analysis on wash load by Gary Parker (a professor at University of Illinois at Urbana-Champaign) suggests that the wash load cut off should decrease in size with increasing sediment load due to damping of turbulent energy by the high concentration of fines. It is possible that damping of turbulent energy may have also contributed to the reduction in the presence of sand in suspension for the higher flows. Further experimental and theoretical analysis should be performed to determine whether or not the observed fining of the suspended load with discharge were an experimental artifact or a physical occurrence. If it is found to be a physical occurrence, then a full mechanistic explanation of the phenomena should be sought.

References

Andrews, E. D. (1980). Effective and bankfull discharges of streams in the Yampa River basin, Colorado and Wyoming. *Journal of Hydrology*, 46(3-4):311–330.

Asquith, W. H. and Slade, R. M. (1997). Regional equations for estimation of peak- streamflow frequency for natural basins in Texas. Technical report, U.S. Geological Survey Water- Resources Investigations Report 96–4307.

ASTM (2007). ASTM d3977 - 97(2007) standard test methods for determining sediment concentration in water samples. *American Society for Testing and Materials*, 11.02.

Biedenharn, D. S., Copeland, R. R., Thorne, C. R., Soar, P. J., Hey, R. D., and Watson, C. C. (2000). Effective discharge calculation: A practical guide. ERDC/CHL TR-00-15, U.S. Army Engineer Research and Development Center, Coastal and Hydraulics Laboratory.

Brown, C. B. (1950). *Sediment Transportation*. John Wiley & Sons Ltd., New York.

Crowder, D. W. and Knapp, H. V. (2005). Effective discharge recurrence intervals of Illinois streams. *Geomorphology*, 64(3-4):167 – 184.

Davis, B. E. (2005). The US DH-2: A one-liter hand-line isokinetic suspended-sediment/water-quality collapsible-bag sampler. Report SS, U.S. Geological Survey and the Federal Interagency Sedimentation Project, Vicksburg, MS.

Diplas, P., Kuhnle, R., Gray, J., Glysson, D., and Edwards, T. (2008). *Sedimentation Engineering: Processes, Measurements, Modeling, and Practice - Sediment Transport Measurements*, chapter 5, pages 307–353. ASCE Manuals and Reports on Engineering Practice No. 110. American Society of Civil Engineering.

Edwards, T. K. and Glysson, G. D. (1999). Field methods for measurement of fluvial sediment. Techniques of Water-Resources Investigations Book 3, Chapter C2, U.S. Geological Survey, Washington D.C.

Einstein, H. A. (1942). Formulas for the transport of bed load. *Transactions ASCE*, 107:561–573.

Emmett, W. and Wolman, M. (2001). Effective discharge and gravel-bed rivers. *Earth Surface Processes and Landforms*, 26(13):1369–1380.

Engelund, F. and Hansen, E. (1967). *A Monograph on Sediment Transport to Alluvial Streams*. Teknik Vorlag, Copenhagen.

Hey, R. D. (1997). Channel response and channel forming discharge: literature review and interpretation. Final Report U.S. Army Contract Number R&D 6871-EN-01.

Klonsky, L. and Vogel, R. M. (2011). Effective measures of “effective” discharge. *The Journal of Geology*, 119(1):1–14.

Lane, E. W. (1955). The importance of fluvial morphology in hydraulic engineering. *Journal of the Hydraulics Division, Proceedings of the ASCE*, 81(1):1–17.

Lenzi, M., Mao, L., and Comiti, F. (2006). Effective discharge for sediment transport in a mountain river: Computational approaches and geomorphic effectiveness. *Journal of Hydrology*, 326(1-4):257–276.

Ma, Y., Huang, H. Q., Xu, J., Brierley, G. J., and Yao, Z. (2010). Variability of effective discharge for suspended sediment transport in a large semi-arid river basin. *Journal of Hydrology*, 388(3-4):357 – 369.

Mackin, J. H. (1948). Concept of the graded river. *Geological Society of America Bulletin*, 59:463–512.

Pickup, G. and Warner, R. (1976). Effects of hydrologic regime on magnitude and frequency of dominant discharge. *Journal of Hydrology*, 29(1-2):51–75.

Rubey, W. W. (1933). Settling velocity of gravel, sand, and silt particles. *American Journal of Science*, 25(148):325–338.

Sichingabula, H. M. (1999). Magnitude-frequency characteristics of effective discharge for suspended sediment transport, fraser river, british columbia, canada. *Hydrological Processes*, 13(9):1361–1380.

Silverman, B. (1998). *Density Estimation For Statistics & Data Analysis*. Chapman & Hall/CRC.

Soar, P. J. and Thorne, C. R. (2001). Channel restoration design for meandering rivers. Coastal Hydraulic Laboratory ERDC/CHLCR-01-1, U.S. Army Engineer Research and Development Center, Coastal and Hydraulics Laboratory, Vicksburg, MS.

Vogel, R. M., Stedinger, J. R., and Hooper, R. P. (2003). Discharge indices for water quality loads. *Water Resources Research*, 39(10):1273.

Whiting, P. J., Stamm, J. F., and Moog, D. B. (1999). Sediment-transporting flows in headwater streams. *Geological Society of America Bulletin*, 111(3):450–466.

Wolman, M. G. and Miller, J. C. (1960). Magnitude and frequency of forces in geomorphic processes. *Journal of Geology*, 68:54–74.

A Analysis Plots and Tables Using All Suspended Material (Wash Load Included)

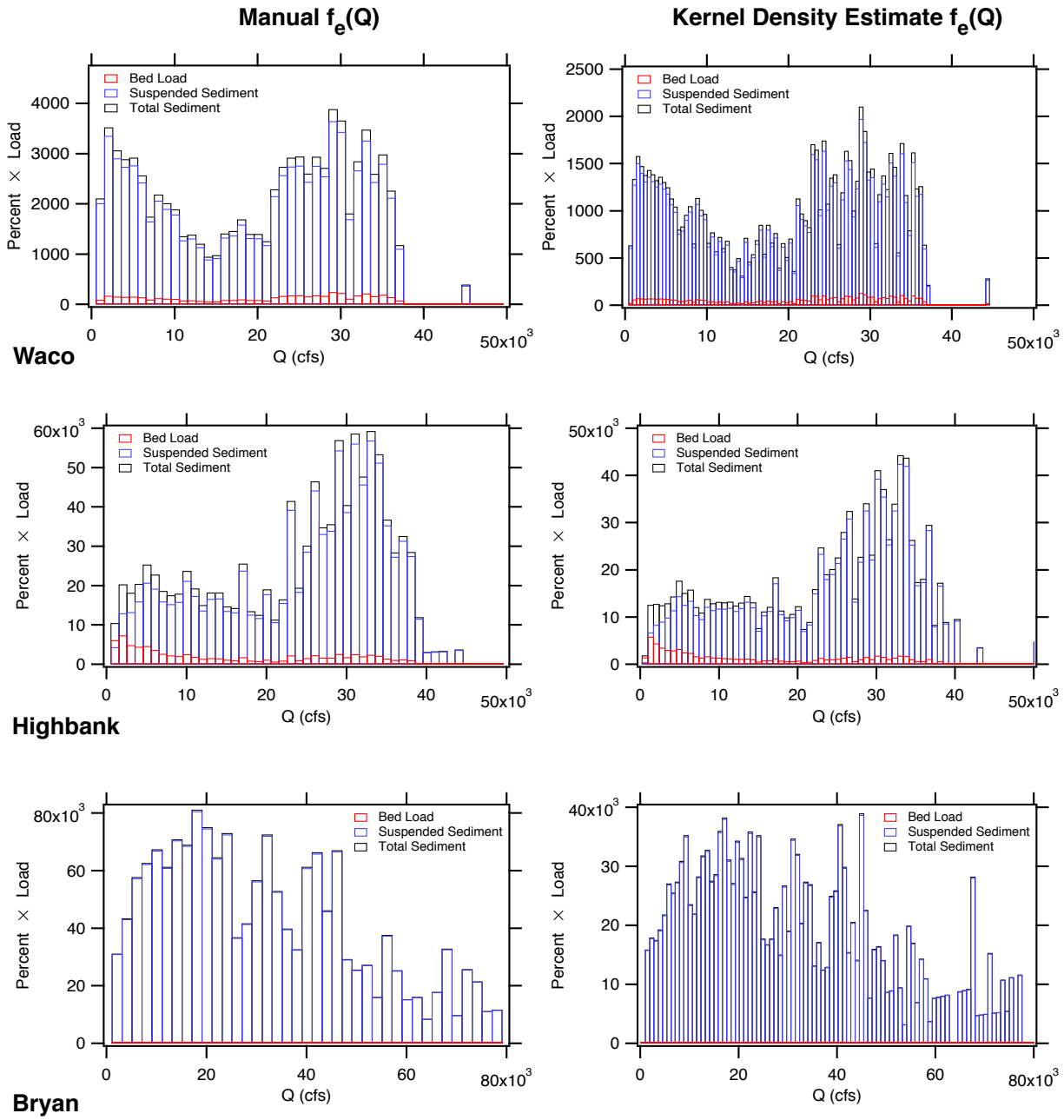

Figure A.1: Sediment transport effectiveness distributions for Waco, Highbank, and Bryan using both the manual and kernel density estimate derived daily flow pdfs.

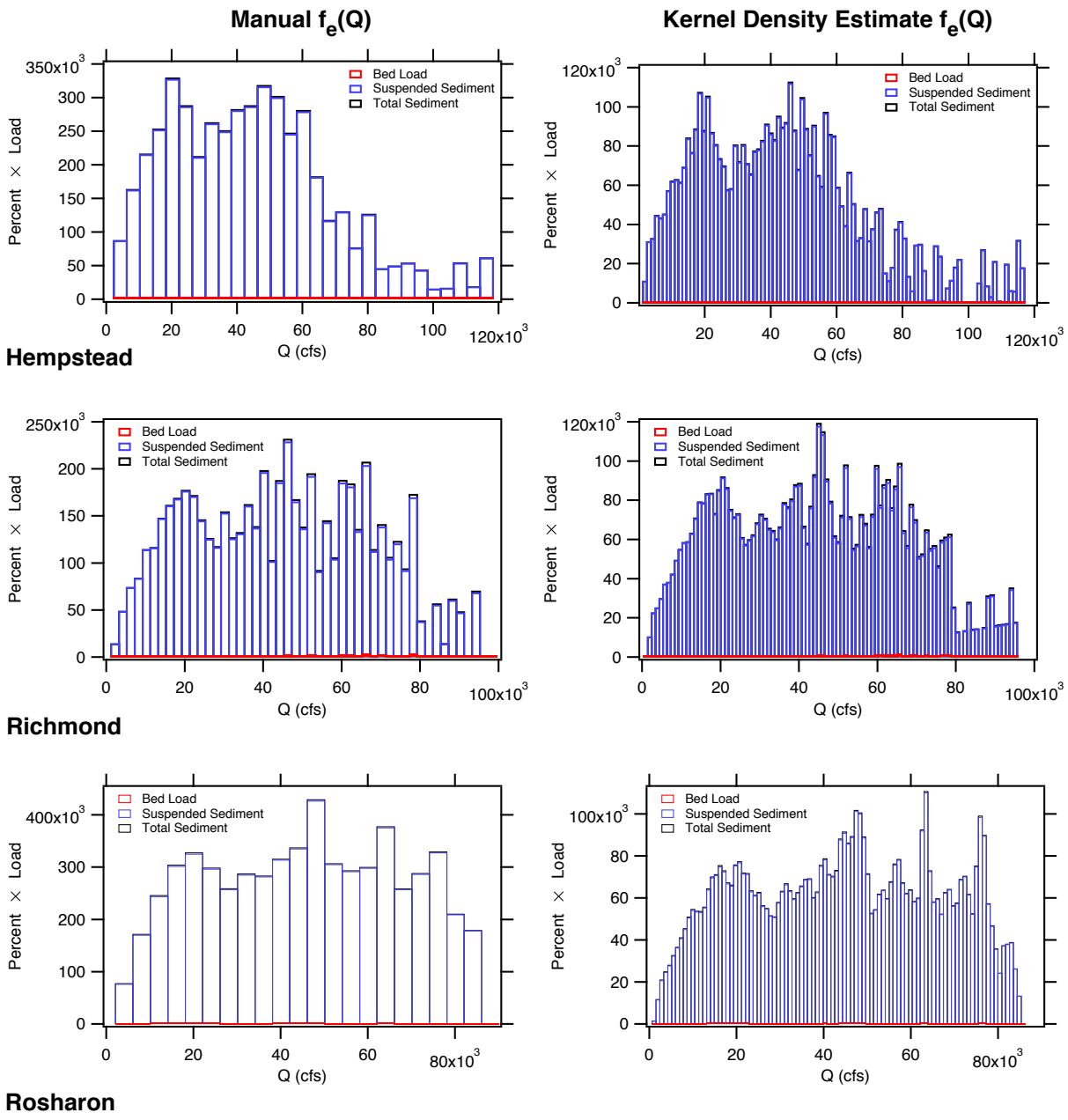

Figure A.2: Sediment transport effectiveness distributions for Hempstead, Richmond, and Rosharon using both the manual and kernel density estimate derived daily flow pdfs.

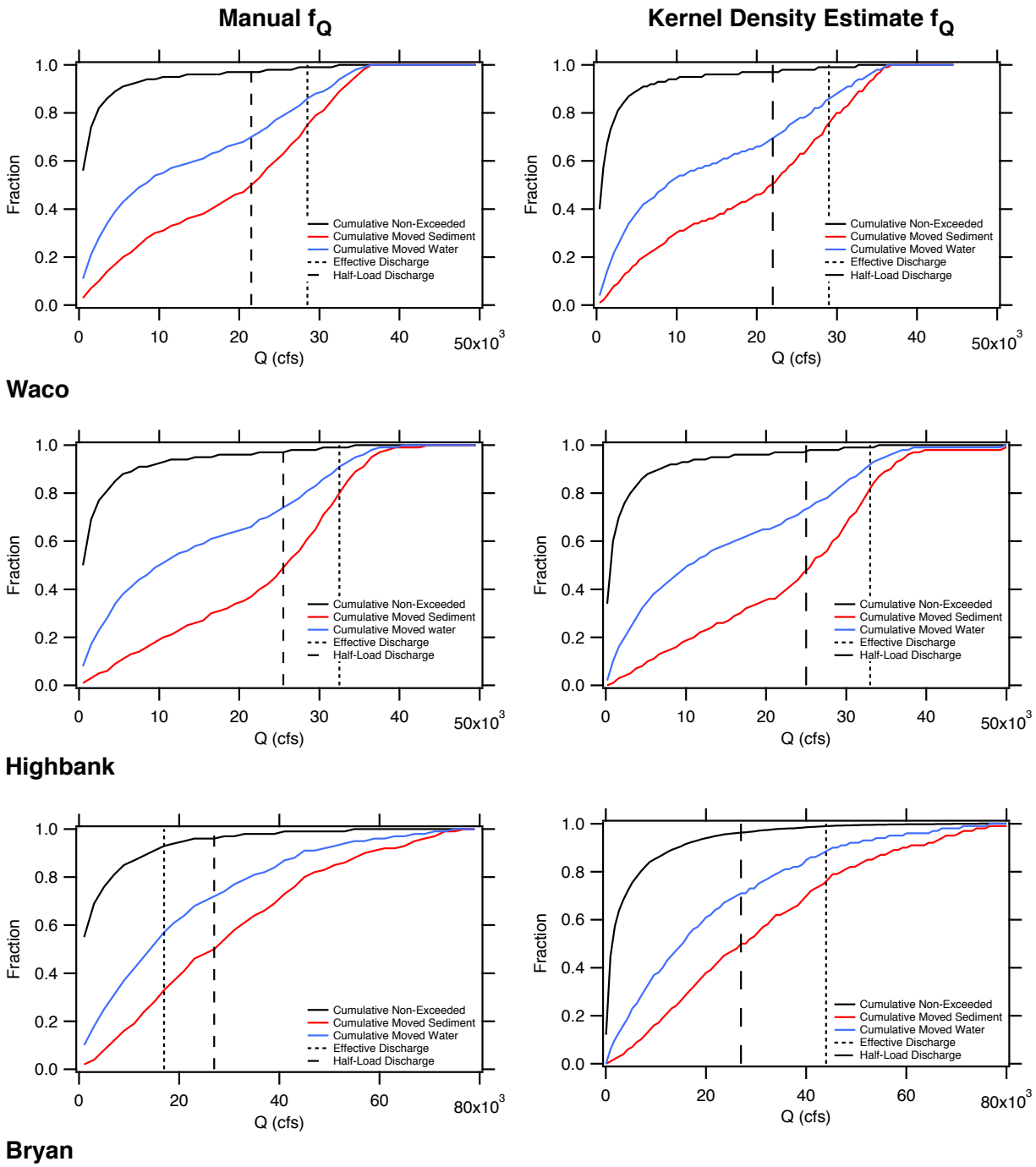

Figure A.3: Summary plots showing the cumulative fraction of flow and sediment moved as a function of discharge, the flow non-exceedance curve, the sediment effective and half-load discharges for Waco, Highbank, and Bryan using the manual and kernel density estimate derived daily flow pdfs.

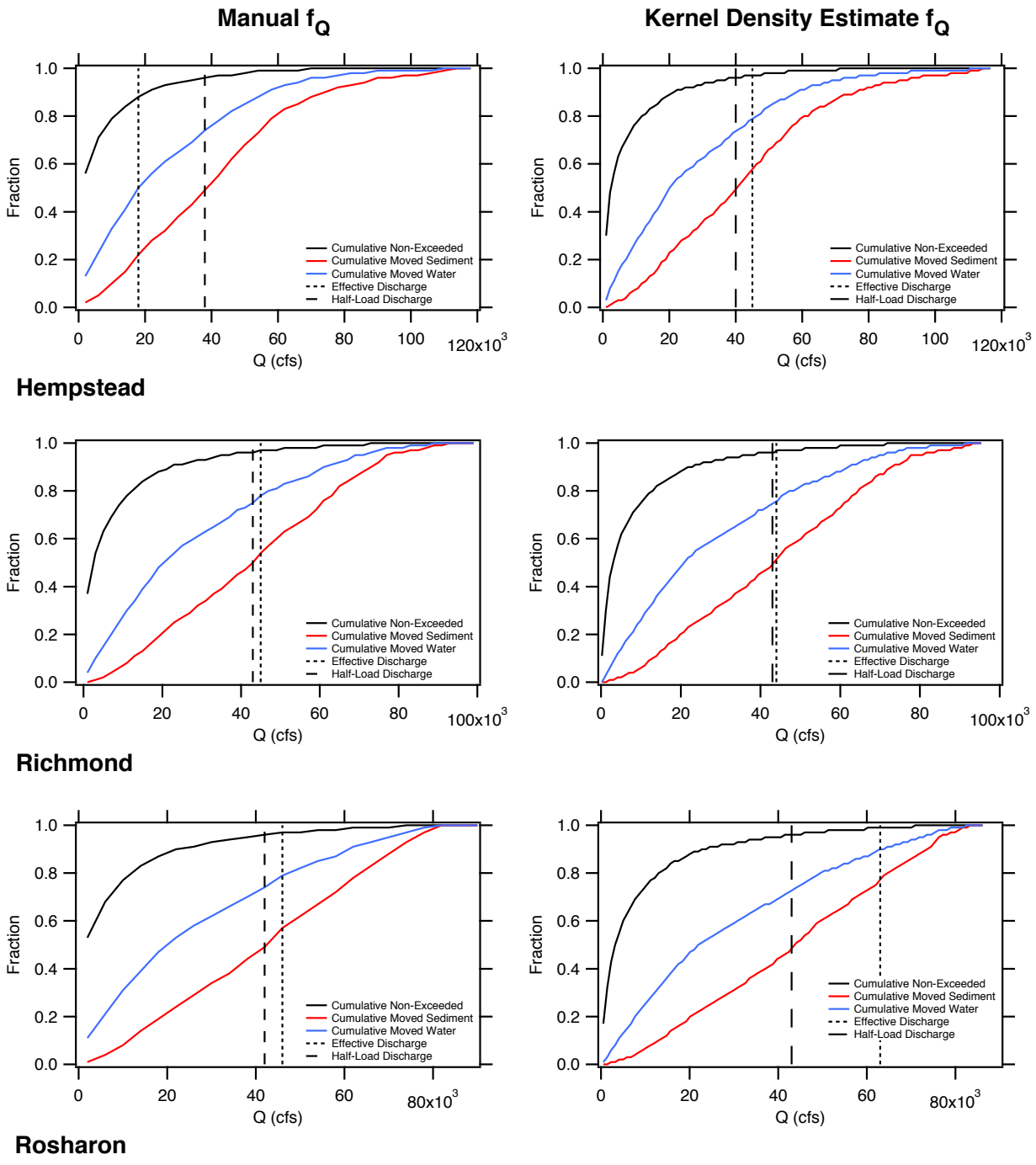

Figure A.4: Summary plots showing the cumulative fraction of flow and sediment moved as a function of discharge, the flow non-exceedance curve, the sediment effective and half-load discharges for Hempstead, Richmond, and Rosharon using the manual and kernel density estimate derived daily flow pdfs.

	Manual $f_e(Q)$					Kernel Density Estimate of $f_e(Q)$				
Station	Q_e [cfs]	$Q_{1/2}$ [cfs]	PT Q_e exceeded	PS carried by $Q < Q_e$	T_R [yr]	Q_e [cfs]	$Q_{1/2}$ [cfs]	PT Q_e exceeded	PS carried by $Q < Q_e$	T_R [yr]
Waco	28500	21500	1	75	2.9	29000	22000	1	74	2.9
Highbank	32500	25500	1	80	2.6	33000	25000	1	80	2.6
Bryan	17000	27000	7	33	1.2	44000	27000	1	77	2
Hempstead	18000	38000	12	22	1.1	45000	40000	3	58	1.5
Richmond	45000	43000	3	54	1.4	44000	43000	3	52	1.4
Rosharon	46000	42000	3	57	1.5	63000	43000	1	77	2.3

Table A.1: Effective discharge summary table. PT: percentage of time that the effective discharge, Q_e is exceeded. PS: percentage of sediment carried by flows less than the effective discharge. T_R: return period of the effective discharge.

	Q_e values using all sediment		Different Q_e values by method?			
Station	Manual [cfs]	Kernel [cfs]	Manual vs Kernel $f_e(Q)$	UH vs USGS+UH	Use of Q_{sbm} vs $Q_{\text{sed-all}}$ Manual	Kernel
Waco	28500	29000	no	-	no	no
Highbank	32500 (32500)	33000 (33000)	no	no	no	no
Bryan	17000	44000	yes	-	no	yes
Hempstead	18000	45000	yes	-	no	yes
Richmond	45000 (65000)	44000 (44000)	no	yes	no	no
Rosharon	46000 (46000)	63000 (63000)	yes	no	no	no

Table A.2: Comparison of calculated effective discharge using both the manual and kernel density estimation for $f_e(Q)$. *Values in parenthesis represent the effective discharge obtained using all of the available USGS data in developing the rating curves at Highbank, Richmond, and Rosharon. The right four columns give an indication of how dependent the calculated Q_e value is on, (1) the method used to develop $f_e(Q)$, (2) whether or not all of the historic USGS data is used in addition to the data measured in this study for suspended bed material, and (3) the use of suspended bed material versus all sediment in suspension (suspended load + wash load) in development of the rating curves.

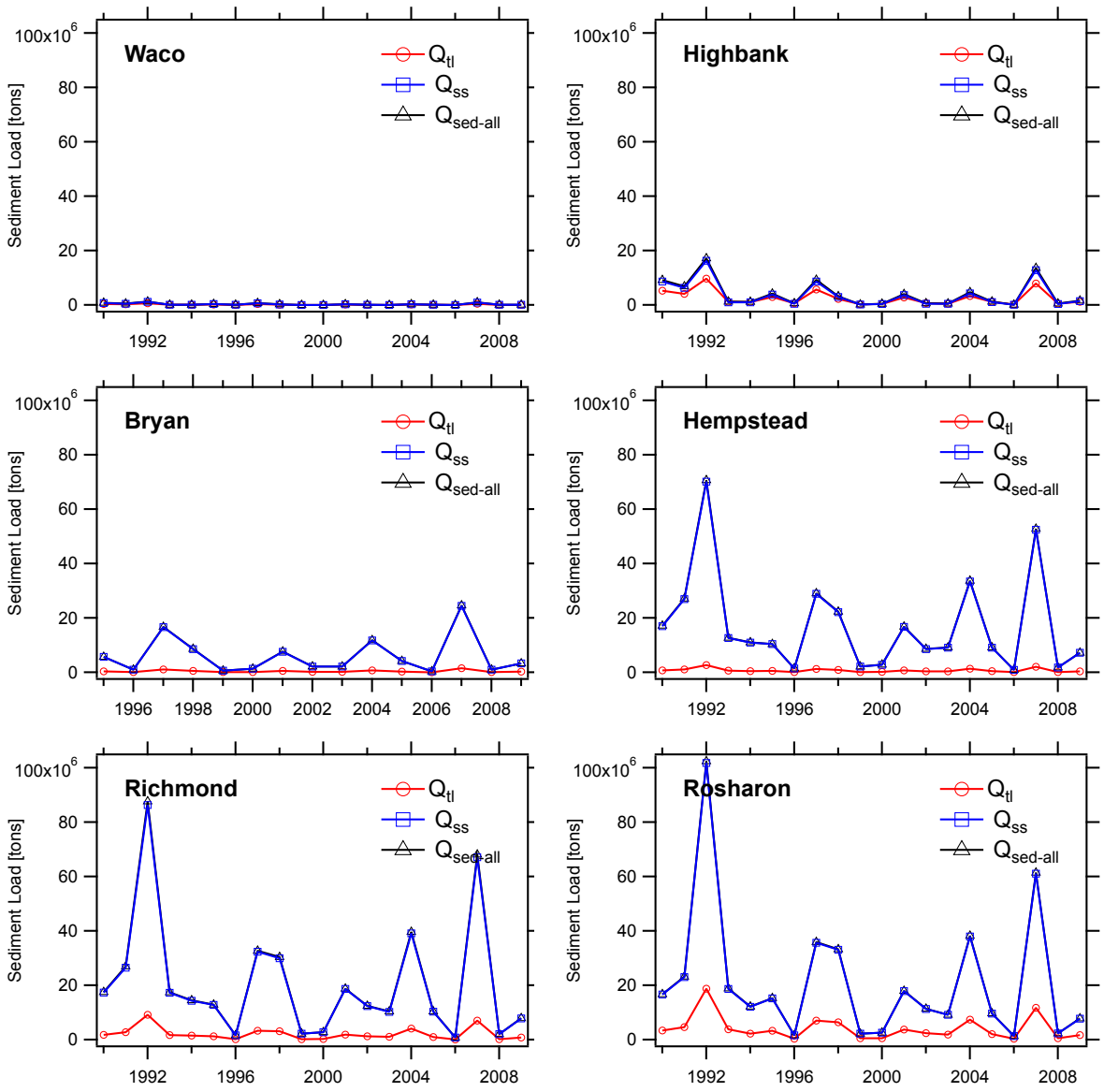

Figure A.5: Yearly total sediments loads at each of the six stations from 1990 through 2009. Q_{tl} is the total bed material load, $Q_{tl} = Q_b + Q_{sbm}$; Q_{ss} is the total sediment load traveling in suspension (suspended + wash load); and $Q_{\text{all-sed}}$ is all of the sediment moving through in both bed and suspended modes, $Q_{\text{sed-all}} = Q_{ss} + Q_b$.